

Determining the Flexural Strength of Asphalt Mixtures using the Bending Beam Rheometer

A THESIS SUBMITTED TO THE FACULTY OF THE GRADUATE
SCHOOL OF THE UNIVERSITY OF MINNESOTA BY

MUGUREL IOAN TUROS

IN PARTIAL FULFILLMENT OF THE REQUIREMENTS
FOR THE DEGREE OF MASTER OF SCIENCE

Dr. MIHAI O. MARASTEANU

December 2010

Acknowledgements

First and foremost, the author would like express his gratitude to his advisor, Dr. Mihai Marasteanu, for his continuous support, sustained encouragement, and valuable advice throughout the study.

The project was greatly enhanced by the gracious assistance of the committee members, Dr. Douglas Hawkins and Dr. Lev Khazanovich.

Thanks also to all colleagues and students who contributed with suggestions.

The Department of Civil Engineering has provided the support and equipment needed to produce and complete this thesis and the University of Minnesota has funded the author's studies.

ABSTRACT

Asphalt mixture creep stiffness and strength are needed in the AASHTO Mechanistic Empirical Pavement Design Guide low temperature algorithm to predict low temperature performance. A procedure for obtaining creep stiffness by testing thin mixture beams using a Bending Beam Rheometer was previously developed at University of Minnesota. The possibility of performing strength tests on thin mixtures beams using a slightly modified Bending Beam Rheometer is investigated in this thesis.

First, standardized strength tests, such as Indirect Tension Test, Thermal Stress Restrained Specimen Test, and Direct Tension Test are performed on a group of eleven mixtures. Then, on the same eleven mixtures, three sets of tests are performed using the proposed method called Bending Beam Strength (BBS).

- The first set of tests is performed to investigate the reliability and reproducibility of BBS testing method, and the validity of the measuring concept. Weibull modulus is calculated as part of the analysis.
- The second set of tests is used to investigate the joint effect of temperature, conditioning time and loading rate, on the measured strength of three different mixtures, by using a 2^3 factorial design
- The third set consists in tests performed on a second group of eight mixtures tested at three temperatures.

The different test results are then compared. Initially the measured values were put side by side. Promising results were obtained but the values were statistically different. The measured values are transformed taking into account the size of the samples and the testing method difference.

The statistical analysis performed on the corrected values show that the BBS strength values are similar to the values obtained with other test methods.

Table of Contents

List of Figures	v
List of Tables	vi
1. Chapter I. Introduction	1
1.1 Background	1
1.2 Objective	1
1.3 Research Approach	1
2 Chapter II. Literature Review	3
2.1 Asphalt Mixture Strength Testing Methods	3
2.1.1 Indirect Tensile (IDT) Test	3
2.1.2 Double Punch Test (DPT).....	6
2.1.3 Direct Tension Test (DTT)	8
2.1.4 Flexural Beam Test (FBT).....	8
2.1.5 Thermal Stress Restrained Specimen Test (TSRST)	9
2.1.6 Summary of Strength Testing Methods	10
2.2 Theoretical Considerations.....	11
2.2.1 General Material Properties	11
2.2.2 Equivalency Relations	12
3 Chapter III. Experimental Work.....	16
3.1 Materials.....	16
3.2 Existing Test Methods.....	18
3.2.1 Indirect Tensile Test	18
3.2.2 Thermal Stress Restrained Specimen Test.....	19
3.2.3 Direct Tension Test.....	21
3.3 New Test Method.....	22
3.3.1 Sample Preparation	23
3.3.2 Equipment.....	23
3.4 BBS Test Matrix.....	25

3.4.1	Weibull Modulus Determination	25
3.4.2	Influence of Loading Rate, Conditioning Time and Temperature on the Test	25
4	Chapter IV. Data Analysis.....	28
4.1	Bending Beam Strength Tests	28
4.1.1	Initial Tests.....	28
4.1.2	Tests for Factors Analysis.....	32
4.1.3	Tests for Strength Comparison	40
4.2	Indirect Tension Test.....	44
4.3	Direct Tension Test	49
4.4	Thermal Stress Restrained Specimen Test (TSRST)	50
4.5	Comparison of the Results from BBS, IDT and DT Testing	50
4.5.1	Measured Values.....	51
4.5.2	Statistical Analysis for the Measured Values	52
4.5.3	Equivalent Values	54
4.5.4	Statistical Analysis for Equivalent Values.....	56
4.5.5	Trend Comparison	58
5	Chapter V. Conclusions	62
	Bibliography	64

List of Figures

Figure 2-1 IDT sample in the loading frame	4
Figure 2-2 Fractured samples showing misalignment effects.....	5
Figure 2-3 Sample geometry.....	5
Figure 2-4 Double punch sample geometry.....	7
Figure 3-1 MTS Testing system	18
Figure 3-2 Thermal Stress Restrained Specimen Test.....	20
Figure 3-3 Hand wheel used to load the sample	21
Figure 3-4 Bending Beam Rheometer with thin asphalt mixture beam.....	22
Figure 3-5 Modified BBR apparatus.....	24
Figure 3-6 Loading rate	26
Figure 4-1 Fracture strength histogram.....	29
Figure 4-2 Scatter plot of fracture strength.....	30
Figure 4-3 Cumulative probability of failure versus fracture strength	32
Figure 4-4 Mixture D maximum bending stress	33
Figure 4-5 Stress strain plots for mixture D.....	34
Figure 4-6 Mixture E maximum bending stress	35
Figure 4-7 Mixture K maximum bending stress	36
Figure 4-8 Maximum bending stress for mixtures A,B,F,G,H,I,L,M.....	42
Figure 4-9 IDT Strength for all mixtures.....	47
Figure 4-10 Strength, measured values.....	52
Figure 4-11 Tensile strength, equivalent unitary volume	55
Figure 4-12 Bland-Altman plot.....	56
Figure 4-13 Strength trend.....	60

List of Tables

Table 2-1 Description of strength tests	10
Table 2-2 Average strength for concrete, different testing methods	11
Table 3-1 Description of the mixtures used for testing.....	16
Table 3-2 Sample description	17
Table 3-3 Summary of IDT tests	19
Table 3-4 Summary of TSRST tests.....	20
Table 3-5 Summary of DTT tests	22
Table 3-6 Summary of initial tests.....	25
Table 3-7 Summary of factor's influence tests.....	26
Table 3-8 Summary of regular condition tests.....	27
Table 4-1 BBS initial results.....	29
Table 4-2 Weibull modulus calculation.....	31
Table 4-3 Mixture D maximum bending stress	33
Table 4-4 Mixture E maximum bending stress.....	34
Table 4-5 Mixture K maximum bending stress	35
Table 4-6 Factors considered for the analysis.....	36
Table 4-7 Input data.....	37
Table 4-8 Least Squares Linear Regression mixture D	38
Table 4-9 Least Squares Linear Regression mixture E.....	38
Table 4-10 Least Squares Linear Regression mixture K	39
Table 4-11 P-values factor effect on the mixture.....	39
Table 4-12 Maximum bending stress for mixtures A,B,F,G,H,I,L,M	40
Table 4-13 Analysis of Variance for maximum bending stress.....	43
Table 4-14 Tukey HSD All-Pairwise Comparisons Test of maximum bending stress for mix	43
Table 4-15 Tukey HSD All-Pairwise Comparisons Test of maximum bending stress for temperature	44
Table 4-16 IDT Strength for all mixtures	45
Table 4-17 Analysis of Variance for IDT Strength	48
Table 4-18 Tukey HSD All-Pairwise Comparisons Test of IDT Strength for mixture	48
Table 4-19 Tukey HSD All-Pairwise Comparisons Test of IDT Strength for temperature	49
Table 4-20 DT Tensile Strength for mixture D,E,K	49

Table 4-21 TSRST Tensile Strength for mixture D,E,K	50
Table 4-22 Fracture Strength, measured values.....	51
Table 4-23 t-Test Paired Two Sample for Means, measured values	53
Table 4-24 Equivalent unitary volume Tensile Strength	54
Table 4-25 t-Test Paired Two Sample for Means, equivalent values	57

Chapter 1. Introduction

1.1 Background

In the northern part of the USA and in Canada, thermal cracking is the main type of distress for asphalt pavements. This type of failure is the result of tensile stresses caused by sudden temperature drops in combination with embrittlement of the asphalt concrete at low temperatures. The Superpave specifications currently used to characterize and select asphalt binder and mixture used in pavement applications include specific test methods for low temperature characterization. These tests are used to determine strength and creep of the asphalt binder and asphalt mixture specimens. Recently a simpler test method was proposed to determine the low temperature creep compliance of asphalt mixtures (1). This thesis takes the previous research one step further, by expanding the previous test method to determine the strength properties for the same materials.

1.2 Objective

The objective of this thesis is to investigate the possible use of a modified Bending Beam Rheometer (BBR) to obtain the flexural strength of asphalt mixtures and to compare the results with the results obtained using other testing methods.

1.3 Research Approach

To accomplish the objective of this thesis, the following approach is used:

- A literature review of the current asphalt mixture strength test methods and of the equivalence methods used for different strength test geometries is performed first.
- Next, an experimental plan is proposed and carried out to obtain relevant data for the analysis
- The analysis is performed using the results obtained with the proposed test method as well as results obtained with other test methods such as Indirect Tensile Test (IDT) (2), Thermal Stress Restrained Specimen Test (*TSRST*) (3) and Direct Tension Test (DTT) (4). Critical issues, such as sample size, loading method, and Weibull modulus, are considered.
- Lastly, a summary and conclusions are provided.

Chapter 2

Literature Review

2.1 Asphalt Mixture Strength Testing Methods

2.1.1 Indirect Tensile (IDT) Test

Known as the “Brazilian” test, the Indirect Tensile Test was developed in 1953 by Carneiro of Brazil (5) and Akazawa of Japan (6). The formulas for estimating the tensile strength and Poisson’s ratio from this test were developed by Hondros (7). During the Strategic Highway Research Program (8), the test was adopted to characterize the resistance of asphalt mixture to low temperature cracking and to predict the performance of the mix (9). The procedure is presented in AASHTO standard T 322-03 (2).

In the IDT strength test, an increasing load is applied along a diametrical plane to the cylindrical specimen to maintain a constant rate of vertical deformation until the specimen fails.

The tensile strength is calculated with the following formula:

$$S_t = \frac{2 \cdot P_f}{\pi \cdot b \cdot D} \quad 2.1$$

where:

S_t = tensile strength, Pa

P_f = failure load, representing the load at which the difference between vertical and horizontal deformation is maximum, N

b = thickness of the specimen, mm

D = diameter of the specimen, mm

To obtain these values, the procedure requires the use of vertical and horizontal LVDTs, mounted on the specimen. Taking in to account the price of these sensors, and the fact that when the specimen breaks they are often damaged or destroyed, many laboratories run the test without the LVDTs. The maximum load is then used to calculate the strength. Following the procedure that uses the failure load offers a better estimate of the tensile strength measured in indirect tension. As a consequence an equation was proposed to correct the strength obtained using maximum load (10):

$$\text{Indirect Tensile Strength} = (0.78 \times \text{IDT Strength}) + 38 \quad 2.2$$

This approach can save expensive instrumentation from destruction, and offers a good estimation of tensile strength. Figure 2-1 represents a picture of the IDT sample in the loading frame.

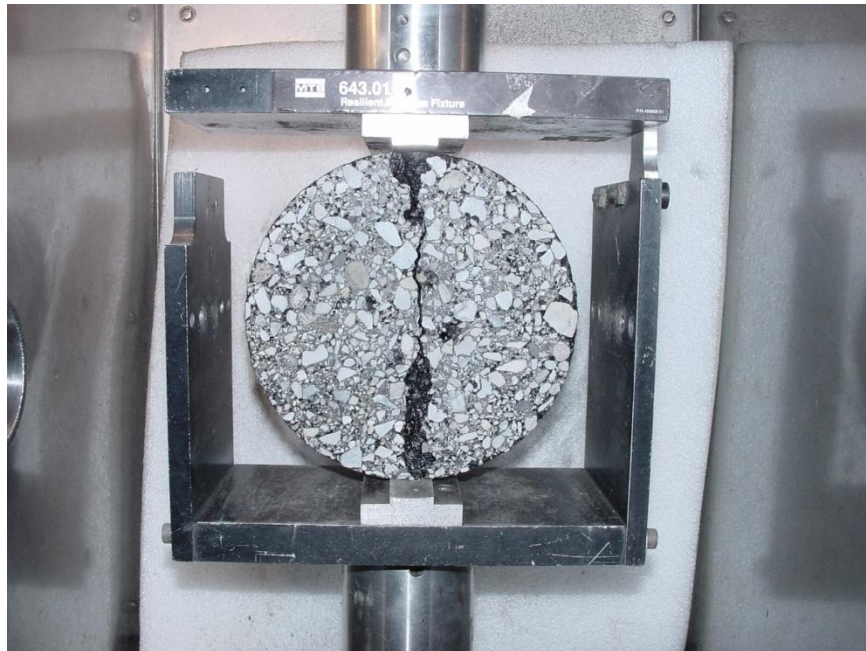


Figure 2-1 IDT sample in the loading frame

During testing, premature failure near the loading points may occur. Generally, load application has to be evenly distributed over the specimen to avoid stress concentration and eccentricities. The curvature of the loading strips is intended to follow the geometry of the specimen, but in fact it causes more problem than it solves unless the curvature and alignment of the specimen perfectly match the loading strip geometry.

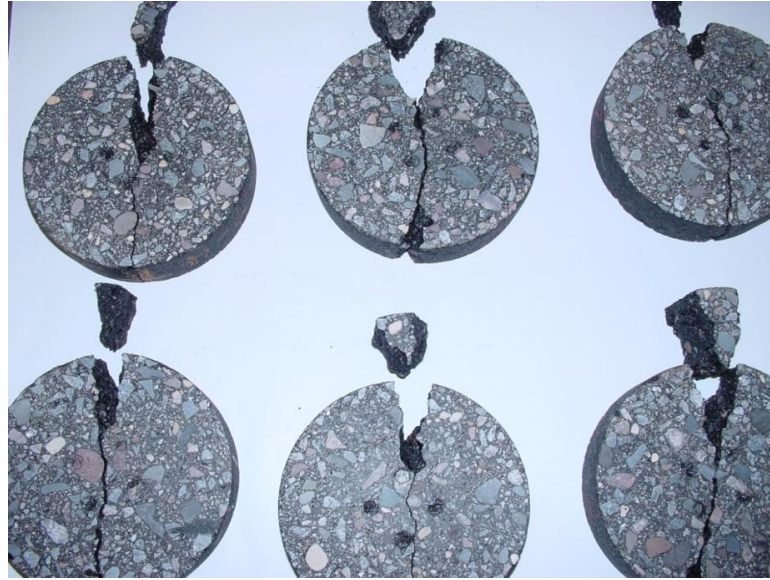


Figure 2-2 Fractured samples showing misalignment effects

A different approach that can eliminate these effects is the use of flat, neoprene loading strips, one half inch thick by one half inch wide (10). These strips follow the exact shape of the IDT specimens, regardless of the irregularities, and greatly reduce the potential for stress concentrations and eccentricities. The sample's dimensions are presented in Figure 2-3 .

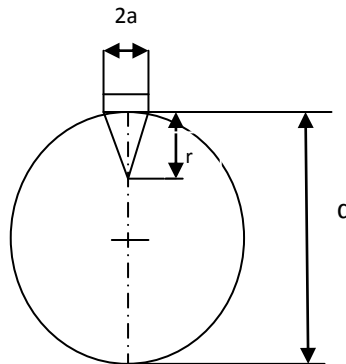


Figure 2-3 Sample geometry

If the load is assumed to be uniformly distributed over the width $2a$, and $2a < 1/10 d$, the stress on the vertical diameter may be adequately approximated by:

Vertical stress:

$$\sigma_r = \frac{2Q}{\pi b D} \left[\frac{d}{4a} (\theta + \sin\theta) + \frac{d}{d-r} - 1 \right] \quad 2.3$$

Horizontal stress:

$$\sigma_\theta = \frac{-2Q}{\pi b D} \left[1 - \frac{d}{4a} (\theta - \sin\theta) \right] \quad 2.4$$

where θ is the angle subtended by the load area at the point considered.

The tensile stress in the central part of the specimen, ($3/4$ of its diameter) remains constant, but changes rapidly to a maximum compressive stress of about 18 times this value under the loading device. The neoprene strips reduce this load peak.

2.1.2 Double Punch Test (DPT)

The double punch test was first developed to determine the tensile strength of concrete (11). Later, it became a test for asphalt mixtures, too (12). Initially, it was used to measure the stripping of the binder from the aggregates (13), (14).

The test is performed by centrally loading a cylindrical specimen, using two cylindrical steel punches placed on the top and bottom surface of the sample. Figure 2-4 presents the geometry and the loading pattern. The specimen is centered between the two 1" punches, perfectly aligned one over the other, and then loaded at a rate of 1"/minute until failure.

The loading condition generate almost uniform tensile stress over the vertical planes containing the load, and the specimen splits across these planes, similarly to the splitting tests.

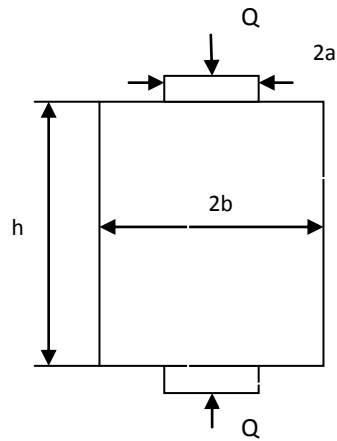


Figure 2-4 Double punch sample geometry

An ideal failure mode for a cylindrical sample tested using this procedure will present several tensile crack planes radiating from a central axis and two cone-shaped rupture regions sheared in the compression zones directly beneath the punches.

The tensile strength is computed by:

$$\sigma_T = \frac{P}{\pi(1.2bh - a^2)} \quad 2.5$$

where:

σ_T =tensile stress, Pa

P= maximum load, N

a= radius of punch, mm

b=radius of specimen, mm

h=height of specimen, mm

Equation 2.5 gives the average tensile stress for the points located in the cracked diametrical planes. More cracked planes indicate more even stress distribution in the test specimen. Most specimens fail in three or four cracks. The plane of failure is not

determinate, so the specimen will fail following the weakest ones. Consequently, consistently lower strengths will be obtained using this test.

2.1.3 Direct Tension Test (DTT)

The direct tension test is performed by applying an axial tensile force to a specimen and measuring the stress strain characteristics of the material (15). The tensile force and the corresponding deformation are recorded and used to calculate the tensile strength and the maximum elongation of the specimen. Gripping the specimen is one of the major problems of this test. A cylindrical or a rectangular specimen is fastened with epoxy to the loading heads. The test is executed with the assumption that only pure tension is applied to the specimen. Bending stresses are produced due to any misalignments and this is the source for errors in the test results. One other assumption for this test is that the stress is uniformly distributed across the central section.

2.1.4 Flexural Beam Test (FBT)

The flexural beam test presents similarities to the real field loading of pavements. In this test a simple supported beam is loaded with either a concentrated force applied at the midpoint or with two equal concentrated forces applied at the two third points of the beam. The testing method has been used to predict the fatigue resistance of asphalt mixtures (16) and to determine the flexural creep stiffness of asphalt binders (17) and asphalt mixtures (18).

For a concentrated load applied at the midpoint, the maximum bending stress occurs at the midpoint of the beam and it is calculated as follows:

$$\sigma = \frac{3PL}{2bh^2} \quad 2.6$$

where:

σ = maximum bending stress in beam, MPa;

P = load, N;

L = span length, mm;

b = width of beam, mm;

h = thickness of beam, mm.

The maximum bending strain is calculated as:

$$\epsilon = \frac{6\delta h}{L^2} \quad 2.7$$

where:

ϵ = maximum bending strain in beam, mm/mm;

δ = deflection of beam, mm;

h = thickness of beam, mm;

L = span length, mm.

2.1.5 Thermal Stress Restrained Specimen Test (TSRST)

This test represents a particular version of the direct tension test. In the TSRST a cylindrical or prismatic specimen is glued to the testing system patterns and the test temperature is lowered at a constant rate while the specimen is continuously loaded axially to keep the height of the specimen constant. The test ends when fracture occurs. The results of this test are a thermal stress versus temperature curve and the stress at failure (3).

The fracture stress is calculated as:

$$\text{Fracture stress} = \frac{P_{ult}}{A} \quad 2.8$$

where:

P_{ult} = ultimate tensile load at fracture in N

A = average cross sectional area in mm²

2.1.6 Summary of Strength Testing Methods

A summary of the tests methods presented above, which includes criteria that can be used to determine advantages and disadvantages for each test, is presented in Table 2-1.

Table 2-1 Description of strength tests

Criteria	IDT	DPT	DTT	FBT	TSRST
Plane of failure	Determined	Not determined	Not determined	Not determined	Not determined
Equipment complexity	High	High	Medium	Low	Medium
Appropriate for field layers tests	Yes	No	No	Yes	Yes

A determined plane of failure does not allow the sample to break on its weakest section, but in a plane determined by the location of the sensors and the sample's position in the testing frame. This will increase the coefficient of variation between replicates and won't offer the most accurate results.

Complex equipment is obviously more expensive, so fewer laboratories will be able to invest in it and to use the testing method for regular investigations.

The typical thickness of asphalt mixture lifts used for paving is 2". Therefore, for forensic investigations, a test that uses a thinner sample will make more sense than one using a thicker one. There are restrictions on how thin a sample can be, mainly due to the aggregate size, but the right balance has to be found.

A comparison of the results obtained using three of these testing methods can be found in (19). A summary of average strength values for Portland cement concrete cylinders are presented in Table 2-2.

Table 2-2 Average strength for concrete, different testing methods

Method	Average strength (psi)	Coefficient of variation (%)
DTT	275	7
FBT	605	6
IDT	405	5

2.2 Theoretical Considerations

2.2.1 General Material Properties

This section briefly addresses theoretical considerations used to evaluate experimental data obtained from different strength testing methods in this thesis.

Linearity

At low temperatures, asphalt mixture is assumed to behave in a linear manner up to the point of failure, due to its high stiffness.

Homogeneity

Homogeneity is the degree to which the properties of the material stay the same at any given location within its boundaries. Asphalt mixture is clearly not homogenous, because it is composed of three distinct elements: aggregate, asphalt binder, and air. This raises questions on whether significant errors are involved in the assumption of analysis of thermal cracking using mechanical methods. The larger a specimen is compared to the contained non-uniformity, the more accurate the assumption on homogeneity is. When a quasi-infinite system, such as a paved road, is analyzed, this is probably a very good assumption. For a laboratory-size specimen, a concept of a representative volume element (RVE) is used (20). RVE represents the minimum acceptable specimen dimension for a given test and material, in order to ensure that the assumption of

homogeneity is met. A simple approach based on geometric analysis and numerical simulations may not be sufficient (21). An alternative is the use of digital-image correlation (DIC) because DIC can capture real-time and continuous variations in deformation and strain of mixture components with high resolution cameras (22).

Anisotropy

Isotropic behavior implies that material properties are independent of direction. Asphalt mixture specimens and pavements are produced through compaction process, in which preferential orientation of the particles occurs. Therefore, the assumption of isotropy is questionable since properties vary depending upon the direction of loading. For example, stiffness in the perpendicular to compaction load was shown to be as high as 30% higher than stiffness in the direction of the compaction. However, stiffness anisotropy decreases with a decrease in the mixture temperature (23). In this thesis, since testing was performed at very low temperatures, asphalt mixtures were assumed isotropic.

Poisson's Ratio

Poisson's ratio represents the absolute value of the ratio of transverse strain to the corresponding axial strain resulting from uniformly distributed axial stress below the proportional limit of the material. In order to analyze IDT creep results (2), it is important to determine strains in both the vertical and horizontal directions and use the results to calculate the Poisson's ratio.

2.2.2 Equivalency Relations

In order to compare equivalent strength values, obtained through different test and for samples having different volumes, two theoretical aspects have to be considered: the size effect and the equivalency between the bending test and the tension test.

2.2.2.1 Size Effect

One aspect that needs to be considered in the data analysis is the statistical size effect, caused by the randomness of material strength. This theory was initially introduced by Weibull in 1939 and is based on the model of a chain (24). The failure load of a chain is

determined by its weakest link. The longer the chain is, the smaller the strength value that is likely to be observed in the chain is. Weibull described this strength behavior using a special form of extreme value distribution, later named Weibull distribution in his honor (25). This results in a definite relationship between mechanical load and the failure probability of the part if the distribution parameters are known. Using a level of strength at which the failure probability becomes 63.2% (σ_0), the Weibull modulus (m) becomes a measure of the distribution of strengths. The higher the Weibull modulus, the more consistent the material (which means that uniform defects are evenly distributed throughout the entire volume), and the narrower the probability curve of the strength distribution. The failure probability is calculated as:

$$P = 1 - \exp \left\{ - \left(\frac{\sigma - \sigma_u}{\sigma_0} \right)^m \right\} \quad 2.9$$

where:

P = failure probability

σ_u = minimum strength, typically $\sigma_u = 0$

σ_0 = location parameter of the Weibull distribution, strength at 63.2% failure probability;

σ = stress

m = Weibull modulus

Since the number of possible defects is dependent on the volume of the part, the volume under load must be taken into account. The strength of large parts is thus less than what is measured on test samples. With large volumes under load, a larger Weibull modulus results in higher load capacity. Using Weibull statistics, the following component strength results from the volume relationship:

$$\sigma_{part} = \sigma_{test\ piece} * \left(\frac{V_{test\ piece}}{V_{part}} \right)^{\frac{1}{m}} \quad 2.10$$

2.2.2.2 The Equivalency between Bending Test and Direct Tension Test

Considering a beam subjected to three points bending, loaded in the middle, the nominal stress is defined as the maximum stress according to elastic bending theory:

$$\sigma_n = \frac{3PL}{2bh^2} \quad 2.11$$

where:

σ_n =nominal stress

P=bending load

L= span length

b=width of beam

h= thickness of beam

The elastic stress distribution varies along the thickness of the beam (Y axis) and the length of the beam (X axis) and is given by:

$$\sigma(x, y, \sigma_n) = \frac{2y}{h} \frac{2x}{L} \sigma_n \quad 2.12$$

Where: x and y are coordinate vectors.

The failure probability for the specified applied nominal stress becomes:

$$\begin{aligned} P_f(\sigma_n) &= 1 - \exp \left[- \int_V c(\sigma(x, y, \sigma_n)) dV(x, y) \right] = \\ &= 1 - \exp \left[- \frac{b}{v_0} \left(\frac{4\sigma_n}{hL\sigma_0} \right)^m \int_0^{\frac{h}{2}} \int_0^{\frac{L}{2}} x^m y^m dx dy \right] = \\ &= 1 - \exp \left[- \frac{V}{4(1+m)^2 v_0} \left(\frac{\sigma_n}{\sigma_0} \right)^m \right] \end{aligned} \quad 2.13$$

Where V= volume of the beam, V=Lhb

The probability of failure for the uniform tension case is given by equation (2.14):

$$P_f(\sigma) = 1 - \exp \left[- \frac{V}{v_0} \left(\frac{\sigma}{\sigma_0} \right)^m \right] \quad 2.14$$

Comparing the expression from the brackets in equations (2.13) and (2.14) it results that, from the statistical point of view, a beam in three point bending configuration is

equivalent to a specimen in direct tension with a volume $4(1+m)^2$ times smaller. Therefore, one can write the following expression relating the mean strength derived from pure bending σ_u^B and for pure tension σ_u , on specimens of the same volume:

$$\frac{\sigma_u^B}{\sigma_u} = [4(1 + m)^2]^{\frac{1}{m}} \quad 2.15$$

Chapter 3 Experimental Work

The materials, the testing methods, and the testing matrix pursued in the experimental investigation are presented in the next paragraphs.

3.1 Materials

Eleven asphalt mixtures produced using different asphalt binders, aggregates, and containing various amounts of reclaimed asphalt pavement (RAP) and roofing shingles were used in the experimental work. These materials were used in the 2008 reconstruction of test cells at MnROAD facility. Loose asphalt mixture was sampled from the cells.

Table 3-1 summarizes the materials used.

Table 3-1 Description of the mixtures used for testing

Material	Mix type	Description	PG	RAP
A	Novachip		70-28	none
B	SPWEB440F	level 4 Superpave	64-34	none
D	SPWEB440 F Special	4.75 taconite Superpave	64-34	none
E	SPWEB440 C Special	WMA wear course	58-34	up to 20%
F	SPWEB430 C Special	WMA non wear	58-34	up to 20%
G	SPNWB430 B	non wear	58-28	30% non fractioned
H	SPNWB430 B Special	non wear	58-28	30% fractioned
I	SPNWB430 C Special 1	non wear	58-34	30% fractioned
K	SPWEB400B (1)	shoulder mix	58-28	none, 5% manufactured waste shingles
L	SPWEB440C	control for WMA	58-34	up to 20 %
M	SPWEB400B (1)	shoulder mix	58-28	none, 5% manufactured tear off shingles

*WMA – warm mix asphalt

The test specimens were prepared as follows:

- The loose mix, received in 5 gallons buckets was heated in an electrical oven at 135 °C;
- 150 mm by 170 mm height cylinder were compacted using a Brovold Gyrotory Compactor to a 7% air void content;
- The top 12 mm and the bottom 12 mm of the gyrotory specimen were removed using a typical laboratory saw to obtain smooth surfaces
- Testing specimens were cut from the gyrotory cylinders

Additional details are provided in the section describing the test method used.

Table 3-2 below provides a summary of the test specimens used in the experimental work.

Table 3-2 Sample description

Test	Sample			
	Shape	Size	Volume	Weight
IDT	cylindrical	D: 150 mm, H: 40mm	706 cm ³	1765g
DT, TSRST	cylindrical	D: 50.8mm, H: 150mm	303 cm ³	760 g
BBS	rectangular	L: 120mm, H:6.5mm, W:12.5mm	9.7 cm ³	24 g

An additional cylinder was used for the initial tests and for the Weibull modulus determination. It was compacted using a PG 58-28 binder, granite aggregates at a 4% air void.

3.2 Existing Test Methods

3.2.1 Indirect Tensile Test

The testing method was described in paragraph 2.1.1.

For this experimental work 40 mm thick slices were obtained by cutting each cylinder with a table saw. For testing a floor standing MTS servo-hydraulic testing system (Figure 3-1) was used. It is equipped with a 100 KN load cell, an environmental chamber that keeps the desired testing temperature with an accuracy of $\pm 1^{\circ}\text{C}$, a cooling system using liquid nitrogen, a Eurotherm temperature controller, a data acquisition system, and a loading frame (2). As the picture shows this is a costly complex piece of equipment and requires for conditioning liquid nitrogen tanks.



Figure 3-1 MTS Testing system

After a 2 hours conditioning time, IDT Strength tests were run without using extensometers, and without using neoprene strips. The displacement rate of the loading cross head was 12.5 mm/min, as described in AASHTO IDT standard (2).

The test matrix for the 11 materials described in Table 3-1 is presented in Table 3-3.

Table 3-3 Summary of IDT tests

Material	Temperature (°C)	Number of replicates
A	-6; -18; -30	3/temperature
B	-12; -24; -36	3/temperature
D	-12; -24; -36	3/temperature
E	-12; -24; -36	3/temperature
F	-12; -24; -36	3/temperature
G	-6; -18; -30	3/temperature
H	-6; -18; -30	3/temperature
I	-12; -24; -36	3/temperature
K	-6; -18; -30	3/temperature
L	-12; -24; -36	3/temperature
M	-6; -18; -30	3/temperature

3.2.2 Thermal Stress Restrained Specimen Test

The testing method is described in paragraph 2.1.5.

From each cylinder two cores with a 2” diameter were extracted. After removing the top 10 mm and the bottom 10 mm using a typical laboratory saw, a 150 mm tall, 50.8mm diameter cylinder with two smooth and parallel surfaces is obtained. This was later glued to the testing aluminum plates, using an epoxy resin.

The machine includes a load/displacement system, a cooling system and an acquisition system.

Two Invar rods and two LVDTs are attached to opposite ends of the specimen platens. As the specimen begins to contract, the Invar rods depress the tips of the LVDTs, sending a displacement signal to the test control/data acquisition system. When the average of the two LVDT readings indicates the specimen contracted more than 0.0001 inch, the computer controlled step motor stretches the specimen back to its original length.

The load cell measures the tensile load applied to the specimen. Figure 3-2 presents the sample setup, instrumented with the LVDTs, Invar rods and thermocouples after the failure occurred.



Figure 3-2 Thermal Stress Restrained Specimen Test

Due to low availability of material, only three mixtures, D, E, and K from Table 3-1 were tested using this method. Two replicates were used for each mixture. It was observed that fracture took place at a higher temperature than the lowest temperature used to test the mixtures in other tests. Table 3-4 summarizes the TSRST test matrix.

Table 3-4 Summary of TSRST tests

Material	Number of replicates
D	2/temperature
E	2/temperature
K	2/temperature

3.2.3 Direct Tension Test

The testing method is described in paragraph 2.1.2.

The sample preparation was identical to the TSRST preparation and the TSRST machine was used for testing. However, testing was performed using a time consuming but innovative approach that allows running DT experiments without any modification to the TSRST machine.

The specimen was not instrumented with the invar rods. Instead, it was cooled to the testing temperature and maintained for thermal equilibration in an unloaded state. The tensile force was applied manually, by rotating a hand wheel (Figure 3-3). The circumference of the hand wheel was divided in 36 sectors. Every 30 seconds the hand wheel was indexed with one sector. From the machine's instructions, it was known that one complete rotation of the wheel translates in a 0.01" vertical displacement of the upper plate. These values were selected in order to have an upper plate displacement rate comparable with the strain rate in the BBS.

The data acquisition system recorded the load at failure.

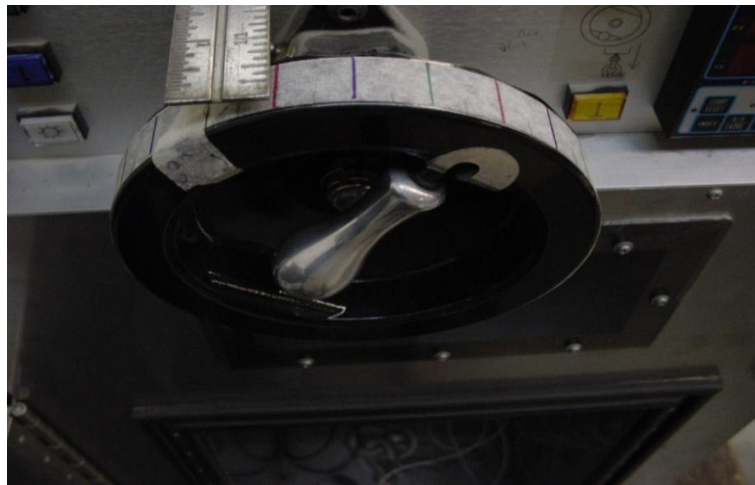


Figure 3-3 Hand wheel used to load the sample

Similar to TSRST, only three mixtures, D, E, and K were tested. Two replicates and one temperature, the lowest one, were used for each mixture. Table 3-5 summarizes the DDT test matrix.

Table 3-5 Summary of DTT tests

Material	Temperature (°C)	Number of replicates
D	-36	2/temperature
E	-36	2/temperature
K	-30	2/temperature

3.3 New Test Method

As mentioned before, the standard test method to determine low temperature properties of asphalt mixtures is the Indirect Tension Test (2) used to perform creep and strength tests on cylindrical specimens loaded in compression along the diameter. Recently, a much simpler and less expensive approach was proposed to determine creep stiffness (18). Thin asphalt mixture beams were tested in a Bending Beam Rheometer (BBR) in order to determine the creep properties (Figure 3-4).

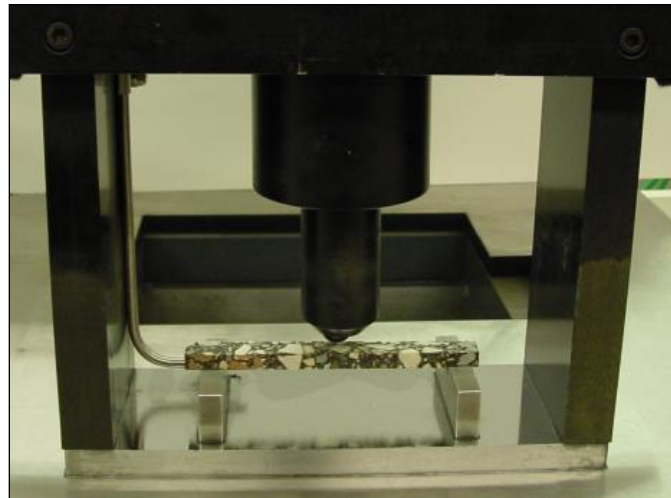


Figure 3-4 Bending Beam Rheometer with thin asphalt mixture beam

The experimental data obtained for 20 laboratory mixtures, was used in a statistical analysis that showed that the BBR and IDT creep stiffness results were not significantly different.

The next logical step was to develop a method to perform a strength test using the same thin mixture beams specimen and the Bending Beam Rheometer. The creep and strength

stiffness of asphalt mixtures represent the two critical parameters required in the Mechanistic-Empirical Pavement Design Guide (MEPDG) to predict low temperature cracking performance.

The new test method will be referred to as Bending Beam Strength (BBS) from this point.

3.3.1 Sample Preparation

Each cylinder was cut into three 40 mm and one 12.5 mm thick slices. The 40 mm are used for the IDT. The 12.5 mm is cut to obtain thin rectangular beams, with a length $L=120\text{mm}$, thickness $h=6.5\text{ mm}$ and width $w=12.7\text{ mm}$. First three cuts are done to obtain a 122mm wide irregular slice. Further 6.5 mm thin beams are cut using a tile saw with a continuous rim blade. Eleven beams are obtained from each slice and are stored on a plane surface and labeled before testing

3.3.2 Equipment

A slightly modified Bending Beam Rheometer (26) test system was used to perform the strength test. The modifications were as follows:

- The 9800mN load cell was replaced by Cannon Instrument Company, the manufacturer of the device, with a 45000mN cell to be able to accurately measure the higher loads required to break the thin mixture beams.
- The air bearing system was used to provide the seating and contact load. However, the test load that is not constant in this test and increases with time, was applied through an added external system.
- A 4 liter plastic container was attached, to the existing loading platform, using steel stripes. (see Figure 3-5)
- A small centrifugal pump, with a volumetric flow rate of 4 liters/minute at a total static head of 1 meter was used to fill the container with water. The flow was restricted by using calibrated ends inserted in the hose. Different flow rates (loading rates) were obtained by using different ends.

- A larger bucket, in which the pump is immersed, was used to keep constant the height difference between the surface of water in it, and in the plastic container. This allowed raising the load from the initial value (the contact load set at 35mN) to 40000mN during the test.
- The test ends when the asphalt mixture beam breaks.



Figure 3-5 Modified BBR apparatus

The dimensions of the beams were recorded with higher accuracy. Because power two of the thickness is used in computation, a small error of 0.2mm will change the calculated value for the stress by 10%. To minimize this, the thickness and the width were measured in three points along the length of the beam and the average values were used in calculation.

3.4 BBS Test Matrix

3.4.1 Weibull Modulus Determination

To check the performance of the testing method, and to determine Weibull modulus a set of 26 tests was run. All the beams were cut from the additional cylinder described before in paragraph 3.1. Because the eleven mixtures used in the test have different properties it was preferred to run the Weibull modulus tests on an average material, commonly used by MNDOT.

The beams were conditioned for 1 hour at -24°C and the “low” loading rate was used. The loading rate factor is described in paragraph 3.4.2. The parameters of the test are presented in Table 3-6.

Table 3-6 Summary of initial tests

Material	Temperature (°C)	Conditioning time (hour)	Loading rate (mN/min)	Number of replicates
PG 58-28 mix	-24	1	3000	26

3.4.2 Influence of Loading Rate, Conditioning Time and Temperature on the Test

Three different materials, D, E, K, presented in Table 3-1 were used to investigate the effect of loading rate, conditioning time, and testing temperature.

Two levels were used for the loading rate. For the “low” level, the load increases from 0 mN to breaking point at a nominal rate of 3000mN/min. For the “high” level, the load increases from 0 mN to breaking point at a nominal rate of 13000mN/min. The rate was kept constant during the test, as shown in Figure 3-6.

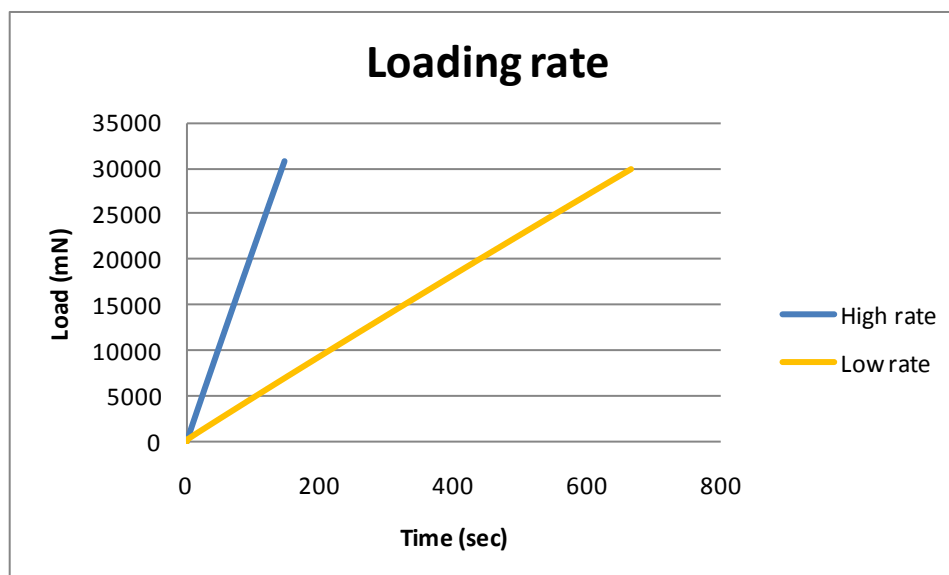


Figure 3-6 Loading rate

The reason for using two different loading rates was to investigate relaxation effects during the test.

Two conditioning periods were used for testing: the first one was 1 hour, similar to binder testing, (17) and the second one was 24 hours to investigate physical hardening effects over longer conditioning times.

The testing temperature was selected according to the PG grade of the binder used in each mixture. A higher temperature (PG +22)^{°C}, intermediate (PG +10)^{°C}, and lower temperature (PG -2)^{°C} were calculated. For the group of three mixtures, testing was performed at lower and intermediate temperature.

Three replicates were tested for each set of factors, for a total 24 tests for each material.

The setup for the test is presented in Table 3-7.

Table 3-7 Summary of factor's influence tests

Material	Temperature (°C)	Conditioning time (hour)	Loading rate (mN/min)	Number of replicates
D	-24; -36	1 hour; 24 hours	3000; 13000	3/set of factors
E	-24; -36	1 hour; 24 hours	3000; 13000	3/set of factors
K	-18; -30	1 hour; 24 hours	3000; 13000	3/set of factors

The other 8 materials presented in Table 3-1 were tested under regular conditions, this means a 1 hour conditioning time, low loading rate and three replicates per temperature. The testing temperature was selected according to the PG grade of the binder used in each mixture. A higher temperature (PG +22)°C, intermediate (PG +10) °C , and lower temperature (PG -2) °C was used. The setup for this test is presented in Table 3-8.

Table 3-8 Summary of regular condition tests

Material	Temperature (°C)	Conditioning time (hour)	Loading rate (mN/min)	Number of replicates
A	-6; -18; -30	1	3000	3/temperature
B	-12; -24; -36	1	3000	3/temperature
F	-12; -24; -36	1	3000	3/temperature
G	-6; -18; -30	1	3000	3/temperature
H	-6; -18; -30	1	3000	3/temperature
I	-12; -24; -36	1	3000	3/temperature
L	-24; -36	1	3000	2/temperature
M	-6; -18; -30	1	3000	3/temperature

Chapter 4

Data Analysis

The following analyses were performed on the results obtained in the experimental work presented in chapter 3:

- Investigate the reliability and reproducibility of BBS testing method, and the validity of the measuring concept. Weibull modulus was calculated as part of the analysis;
- Run a 2^3 factorial design to study the joint effect of temperature, conditioning time and loading rate, on the measured strength of three different mixtures; (27)
- Compare the measured values for strength obtained using BBS method with the measured values obtained using other testing methods for eleven different mixtures;
- Transform the measured values for strength obtained using BBS and other methods using equation 2.10 for size effect and equation 2.15 for equivalency between bending stress and tensile stress, and compare them.

4.1 Bending Beam Strength Tests

4.1.1 Initial Tests

To check the performance of the method, a set of 26 beams, described in paragraph 3.4.1, was tested. The testing temperature was -24°C , conditioning duration was 1 hour, and the “low” loading rate $3000\text{mN}/\text{min}$ was used. Table 4-1 below presents the fracture strength for the tested beams:

Table 4-1 BBS initial results

Beam number	Fracture strength, MPa	Beam number	Fracture strength, MPa
1	6.92	14	6.69
2	7.87	15	6.93
3	6.58	16	6.82
4	7.30	17	6.62
5	7.56	18	7.72
6	7.05	19	6.66
7	7.17	20	6.61
8	6.24	21	7.48
9	7.35	22	7.19
10	5.72	23	6.83
11	7.15	24	7.41
12	7.35	25	6.21
13	6.65	26	5.35

The histogram of failure results presented in Figure 4-1 shows the distribution of fracture strength. It is not symmetrical and is skewed to the right. The lower fracture strength values correspond to the weaker samples.

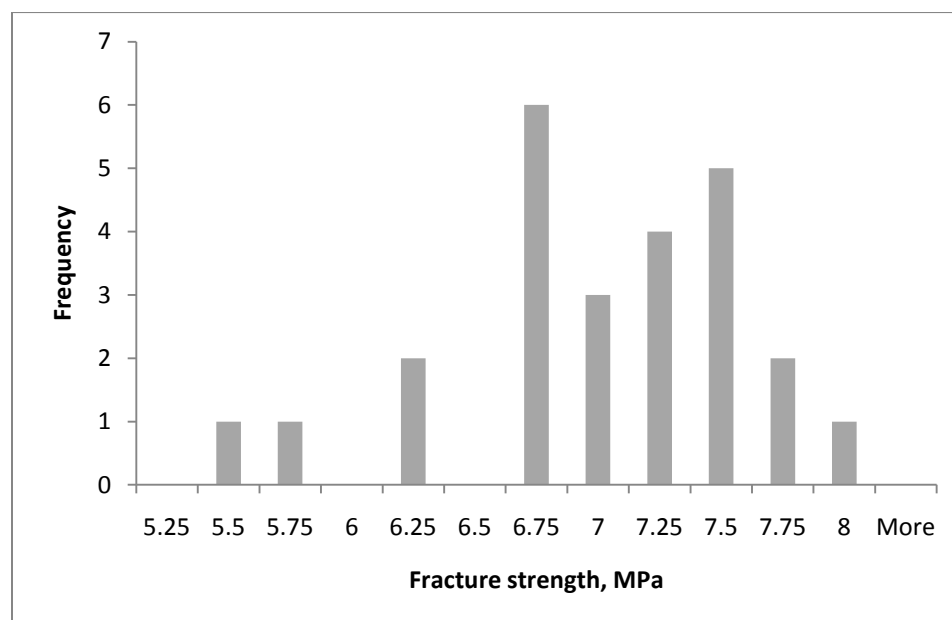


Figure 4-1 Fracture strength histogram

The same data is presented in Figure 4-2 in the form of a scatter plot to check for outliers. It presents a wide distribution of the results, but there are no clear outliers.

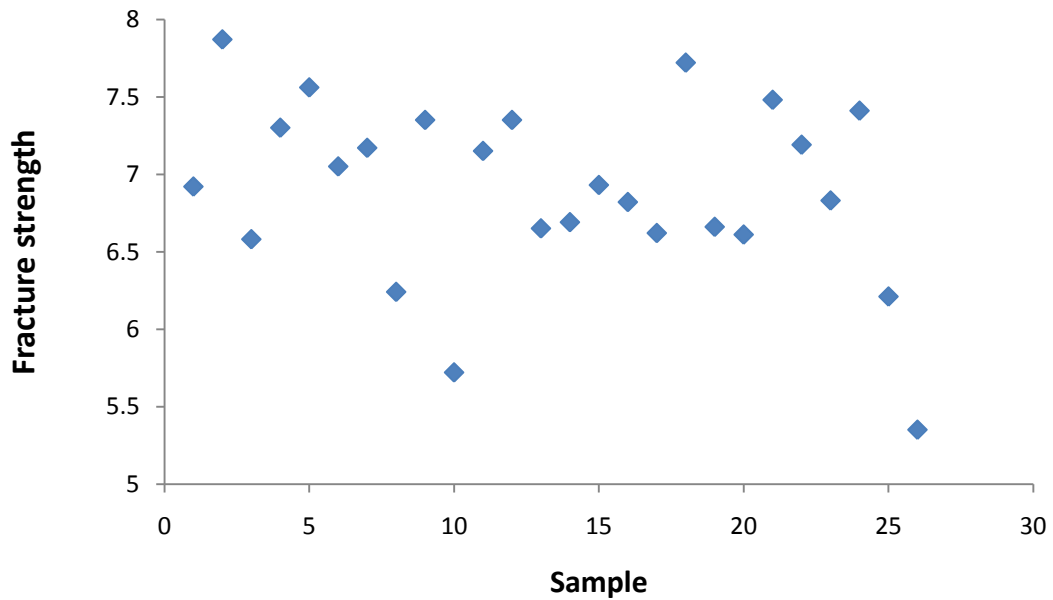


Figure 4-2 Scatter plot of fracture strength

The same set of data presented in Table 4-1 was used to calculate the Weibull modulus, m :
(28)

$$m = \frac{\ln \sigma - \ln \sigma_0}{\ln \left(\ln \left(\frac{1}{1-F(V)} \right) \right)} \quad 4.1$$

The probability of failure for each beam's fracture strength is presented in Table 4-2

Table 4-2 Weibull modulus calculation

Beam #	Fracture strength	Probability of failure F(V0)	Cumulative probability of failure $\ln(\ln(1/(1-F(V0))))$
1	5.35	0.037	-3.277
2	5.72	0.074	-2.564
3	6.21	0.111	-2.138
4	6.24	0.148	-1.830
5	6.58	0.185	-1.585
6	6.61	0.222	-1.381
7	6.62	0.259	-1.203
8	6.65	0.296	-1.045
9	6.66	0.333	-0.902
10	6.69	0.370	-0.770
11	6.82	0.407	-0.647
12	6.83	0.444	-0.531
13	6.92	0.481	-0.420
14	6.93	0.518	-0.313
15	7.05	0.555	-0.209
16	7.15	0.592	-0.107
17	7.17	0.629	-0.006
18	7.19	0.666	0.094
19	7.30	0.703	0.195
20	7.35	0.740	0.300
21	7.36	0.777	0.408
22	7.41	0.814	0.522
23	7.48	0.851	0.646
24	7.55	0.888	0.787
25	7.72	0.925	0.956
26	7.87	0.962	1.192

The cumulative probability of failure is presented in Figure 4-3. The data can be reasonably fitted by a line.

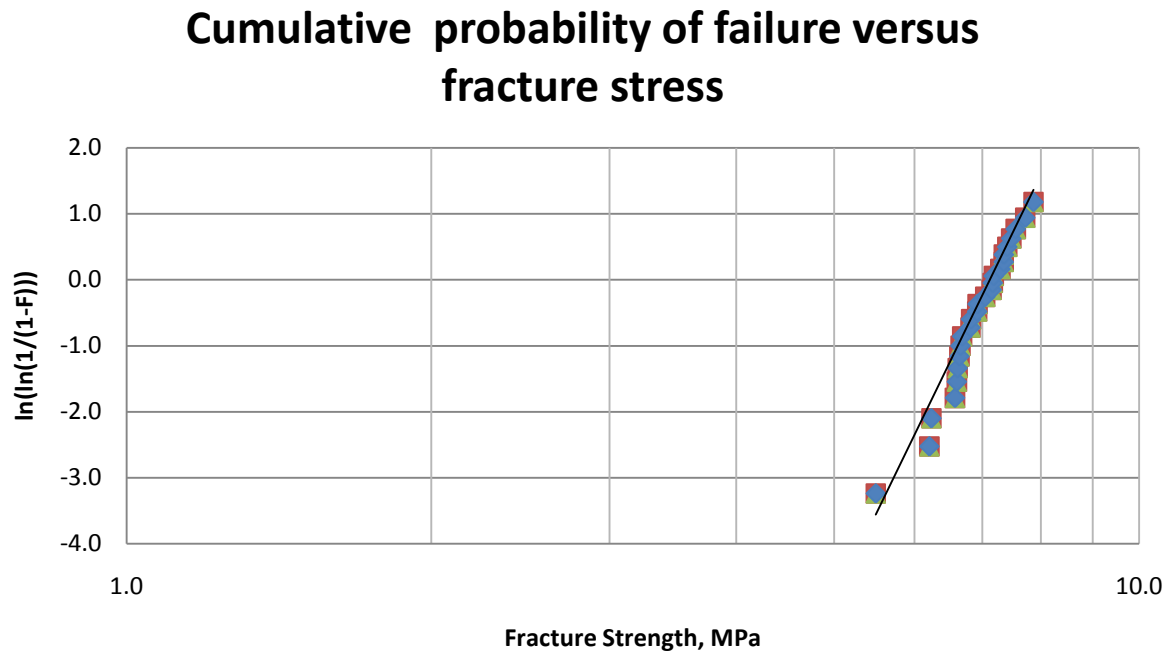


Figure 4-3 Cumulative probability of failure versus fracture strength

The slope of the fitted line is the Weibull modulus, m :

$$m = \frac{1.19266 - (-3.27703)}{\ln 7.86646 - \ln 5.349} = 11.59 \quad 4.2$$

In the literature for a Portland cement concrete the m value was found to be equal to 11. (25)

4.1.2 Tests for Factors Analysis

The influence of three different factors on the testing results was considered. The effect of temperature, conditioning time and loading rate, on the measured strength, was investigated on three different mixtures, type D, E and K presented in Table 3-1. A 2^3 factorial design analysis was run, in order to study the individual and the joint effect of these factors on the fracture strength on beams made from the different mixtures.

Table 4-3 below presents the maximum bending stress for Mixture D, for three replicates, per each set of factors.

Table 4-3 Mixture D maximum bending stress

Maximum Bending Stress (MPa)	Conditioning time/ loading rate/ temperature							
	1h low -24°C	24h low -24°C	1h high -24°C	24h high -24°C	1h low -36°C	24h low -36°C	1h high -36°C	24h high -36°C
Beam #1	10.3	10.5	10.3	9	6.3	9.7	10.8	9
Beam #2	10.5	9.3	10.9	10.9	8.1	8.7	10.5	10
Beam #3	9.2	8.9	9.6	9	7.2	8.7	9.9	9.2

The data was also plotted in Figure 4-4. Visual inspection of the data appears to indicate that the temperature effect is larger than the conditioning time and the loading rate effects.

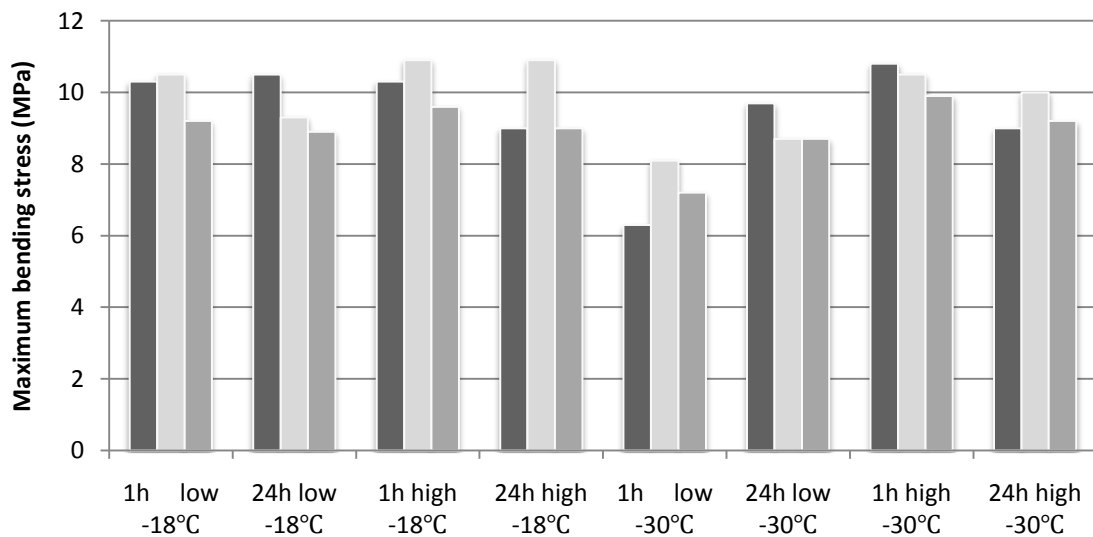


Figure 4-4 Mixture D maximum bending stress

Figure 4-5 below presents the stress strain diagram for Mixture D, tested at -24°C , with a conditioning period of 1 hour, with low and high loading rate. Similar plots were obtained for all tests. It can be seen that the strain is lower for a higher loading rate. This was not investigated in this thesis due to equipment compliance concerns.

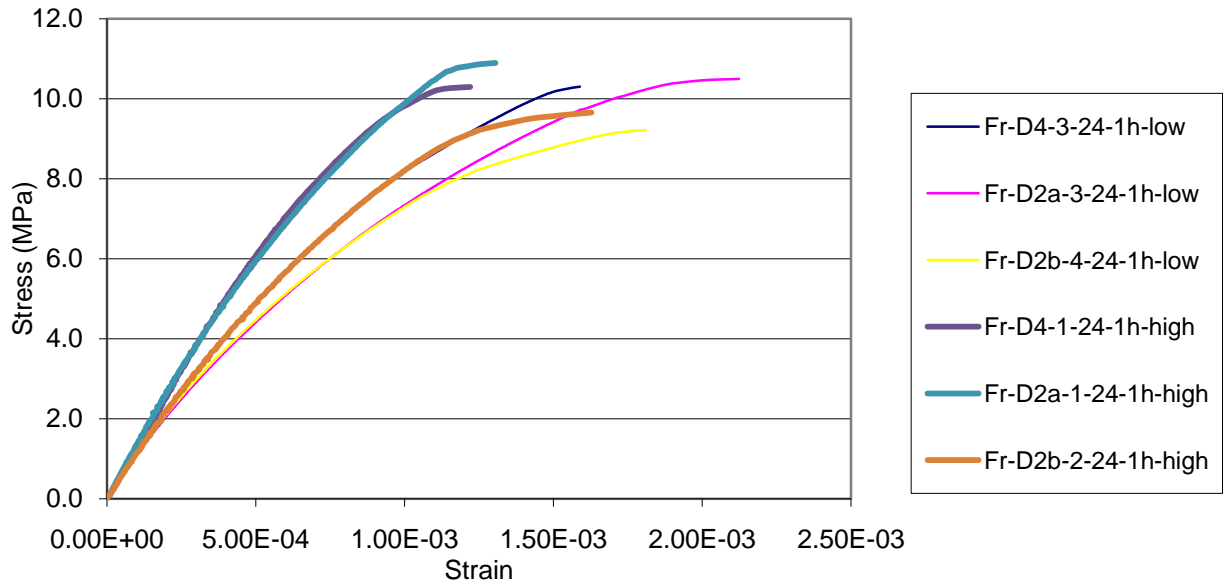


Figure 4-5 Stress strain plots for mixture D

Table 4-4 below presents the maximum bending stress for Mixture E, for the three replicates, for each set of factors. It can be seen from Figure 4-6 that the temperature has a more important influence in decreasing the maximum bending stress, and that the other two factors do not change the measurement result too much.

Table 4-4 Mixture E maximum bending stress

Maximum Bending Stress (MPa)	Conditioning time/ loading rate/ temperature							
	1h low -24°C	24h low -24°C	1h high -24°C	24h high -24°C	1h low -36°C	24h low -36°C	1h high -36°C	24h high -36°C
Beam#1	7.9	7.2	7.5	7	4.7	5.2	5.2	5
Beam#2	6.5	6.9	7.3	5.1	4.3	4.3	5.6	5.9
Beam#3	8	7.1	6.2	7.6	5.1	5.6	4.7	6.4

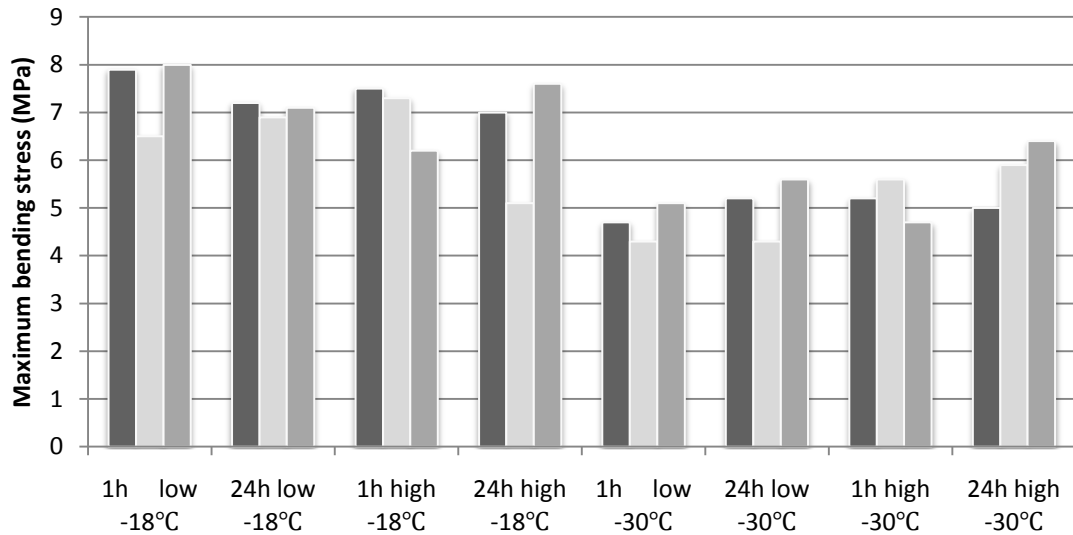


Figure 4-6 Mixture E maximum bending stress

Table 4-5 below presents the maximum bending stress for Mixture K, for the three replicates, for each set of factors. It can be seen from Figure 4-7 a lower influence of the temperature and an alternating effect for the other two factors.

Table 4-5 Mixture K maximum bending stress

Maximum Bending Stress (MPa)	Conditioning time/ loading rate/ temperature							
	1h low -18°C	24h low -18°C	1h high -18°C	24h high -18°C	1h low -30°C	24h low -30°C	1h high -30°C	24h high -30°C
Beam#1	7.4	6.1	6	6.6	4.5	6.5	5.8	4.4
Beam#2	5	5.8	6.3	5.3	4.6	5.1	5.9	5.5
Beam#3	6.6	5.2	5.4	6.2	5.2	6.2	6.9	6

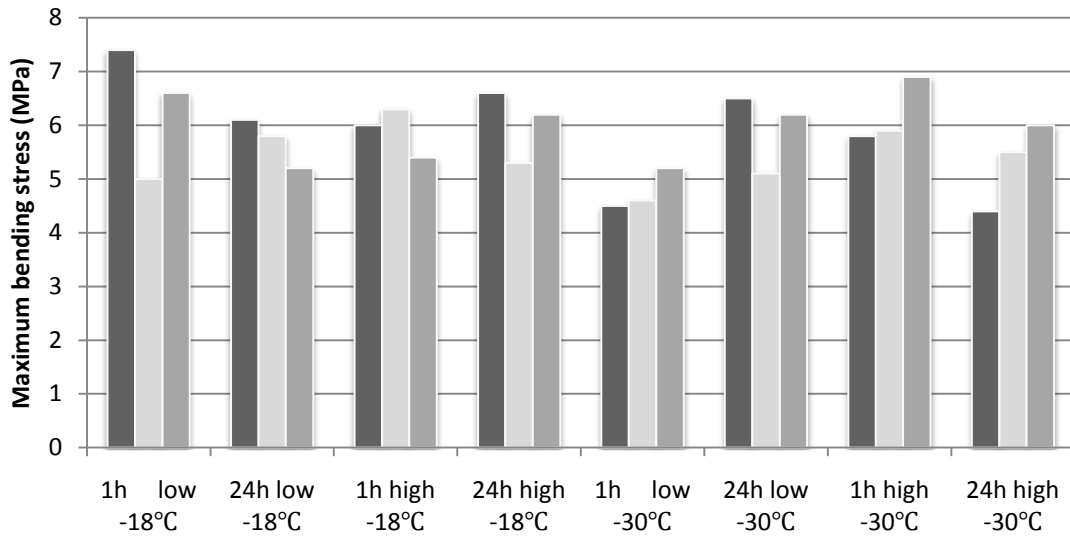


Figure 4-7 Mixture K maximum bending stress

A 2^3 factorial design analysis was also used to study the joint effect of the three factors (temperature, conditioning time and loading rate) on the measured strength on the three mixtures D,E,K. In this analysis each level for each factor is paired with each level for the other factors. By using three factors and two levels the total number of test conditions is $2 \times 2 \times 2 = 8$.

As described before, one hour or 24 hours were used for the conditioning time, a low or a high rate for the loading and two different temperatures, the low or the intermediate. The factors are presented in Table 4-6

Table 4-6 Factors considered for the analysis

Factor		1h/low/low	24h/high/intermediate
X	Conditioning time	-1	1
Y	Loading rate	-1	1
Z	Test temperature	-1	1

To run the analysis, statistical software STATISTIX was used.

Table 4-7 below presents the input data:

Table 4-7 Input data

X	Y	Z	XY	XZ	YZ	XYZ	Stress D	Stress E	Stress K
-1	-1	1	1	-1	-1	1	10.3	7.9	7.4
-1	-1	1	1	-1	-1	1	10.5	6.5	5
-1	-1	1	1	-1	-1	1	9.2	8	6.6
1	-1	1	-1	1	-1	-1	10.5	7.2	6.1
1	-1	1	-1	1	-1	-1	9.3	6.9	5.8
1	-1	1	-1	1	-1	-1	8.9	7.1	5.2
-1	1	1	-1	-1	1	-1	10.3	7.5	6
-1	1	1	-1	-1	1	-1	10.9	7.3	6.3
-1	1	1	-1	-1	1	-1	9.6	6.2	5.4
1	1	1	1	1	1	1	9	7	6.6
1	1	1	1	1	1	1	10.9	5.1	5.3
1	1	1	1	1	1	1	9	7.6	6.2
-1	-1	-1	1	1	1	-1	6.3	4.7	4.5
-1	-1	-1	1	1	1	-1	8.1	4.3	4.6
-1	-1	-1	1	1	1	-1	7.2	5.1	5.2
1	-1	-1	-1	-1	1	1	9.7	5.2	6.5
1	-1	-1	-1	-1	1	1	8.7	4.3	5.1
1	-1	-1	-1	-1	1	1	8.7	5.6	6.2
-1	1	-1	-1	1	-1	1	10.8	5.2	5.8
-1	1	-1	-1	1	-1	1	10.5	5.6	5.9
-1	1	-1	-1	1	-1	1	9.9	4.7	6.9
1	1	-1	1	-1	-1	-1	9	5	4.4
1	1	-1	1	-1	-1	-1	10	5.9	5.5
1	1	-1	1	-1	-1	-1	9.2	6.4	6

The results of the analysis are presented in Table 4-8 for mixture D, Table 4-9 for mixture E and Table 4-10 for mixture K. The main results for this research, the p-values for each factor and combinations of two and three factors are presented in Table 4-11.

Table 4-8 Least Squares Linear Regression mixture D

Predictor					
Variables	Coefficient	Std Error	T	P	VIF
Constant	9.43750	0.15213	62.04	0.0000	0.0
X	-0.02917	0.15213	-0.19	0.8504	1.0
XY	-0.37917	0.15213	-2.49	0.0240	1.0
XYZ	0.32917	0.15213	2.16	0.0460	1.0
XZ	-0.23750	0.15213	-1.56	0.1380	1.0
Y	0.48750	0.15213	3.20	0.0055	1.0
YZ	-0.40417	0.15213	-2.66	0.0172	1.0
Z	0.42917	0.15213	2.82	0.0123	1.0
R-Squared	0.7073	Resid. Mean Square (MSE)			0.55542
Adjusted R-Squared	0.5792	Standard Deviation			0.74526
AICc	7.0131				
PRESS	19.995				
Source	DF	SS	MS	F	P
Regression	7	21.4696	3.06708	5.52	0.0023
Residual	16	8.8867	0.55542		
Total	23	30.3563			
Lack of Fit	0	-3.553E-15	++Inf	-INF	1.0000
Pure Error	16	8.88667	1		
Cases Included 24		Missing Cases 0			

Table 4-9 Least Squares Linear Regression mixture E

Predictor					
Variables	Coefficient	Std Error	T	P	VIF
Constant	6.09583	0.14843	41.07	0.0000	0.0
X	0.01250	0.14843	0.08	0.9339	1.0
XY	0.02917	0.14843	0.20	0.8467	1.0
XYZ	-0.03750	0.14843	-0.25	0.8038	1.0
XZ	-0.22083	0.14843	-1.49	0.1562	1.0
Y	0.02917	0.14843	0.20	0.8467	1.0
YZ	-0.27083	0.14843	-1.82	0.0868	1.0
Z	0.92917	0.14843	6.26	0.0000	1.0
R-Squared	0.7372	Resid. Mean Square (MSE)			0.52875
Adjusted R-Squared	0.6222	Standard Deviation			0.72715
AICc	5.8322				
PRESS	19.035				
Source	DF	SS	MS	F	P
Regression	7	23.7296	3.38994	6.41	0.0010
Residual	16	8.4600	0.52875		
Total	23	32.1896			
Lack of Fit	0	0.00000	-M	NAN-8.76543E0299	
Pure Error	16	8.46000	0.52875		
Cases Included 24		Missing Cases 0			

Table 4-10 Least Squares Linear Regression mixture K

<u>Predictor</u>					
<u>Variables</u>	<u>Coefficient</u>	<u>Std Error</u>	<u>T</u>	<u>P</u>	<u>VIF</u>
Constant	5.77083	0.14583	39.57	0.0000	0.0
X	-0.02917	0.14583	-0.20	0.8440	1.0
XY	-0.16250	0.14583	-1.11	0.2816	1.0
XYZ	0.35417	0.14583	2.43	0.0273	1.0
XZ	-0.09583	0.14583	-0.66	0.5204	1.0
Y	0.08750	0.14583	0.60	0.5569	1.0
YZ	-0.11250	0.14583	-0.77	0.4517	1.0
Z	0.22083	0.14583	1.51	0.1495	1.0
R-Squared	0.4043	Resid. Mean Square (MSE)			0.51042
Adjusted R-Squared	0.1437	Standard Deviation			0.71443
AICc	4.9853				
PRESS	18.375				
<u>Source</u>	<u>DF</u>	<u>SS</u>	<u>MS</u>	<u>F</u>	<u>P</u>
Regression	7	5.5429	0.79185	1.55	0.2203
Residual	16	8.1667	0.51042		
Total	23	13.7096			
Lack of Fit	0	0.00000	-M	NAN-8.76543E0299	
Pure Error	16	8.16667	0.51042		
Cases Included	24	Missing Cases	0		

Table 4-11 P-values factor effect on the mixture

Mix	P-value						
	X	Y	Z	XY	XZ	YZ	XYZ
D	0.85	0.01	0.01	0.03	0.14	0.02	0.05
E	0.93	0.85	0.00	0.85	0.16	0.09	0.8
K	0.84	0.56	0.15	0.28	0.52	0.45	0.03

At 1% level factor Z, the temperature, is significant for mixture D and E. For mixture K the p-value is slightly bigger than 0.01. The only other factor that is significant, but just for one of the mixtures, D, is the loading rate, factor Y. Factor X, conditioning time, does present p-values much bigger than 0.01 for all three mixtures. When the joint effect of two or three factors is considered, none of the combinations present a p-value smaller or equal to 0.01, which means that there is no interaction between the factors.

As a result of this analysis, only one loading rate of 3000 mN/min, and one conditioning time of one hour were considered in the next phase of this investigation. Because the

temperature had a significant effect, further testing was conducted at three different temperatures, based on the PG grade of the binder used in the mixture:

- higher temperature (PG +22)°C
- intermediate temperature (PG +10)°C
- lower temperature (PG -2)°C

Although the factorial analysis does not present huge differences in the behavior of the three different mixtures, the existing dissimilarity may reside in the different design of the mixtures, in terms of binder's composition and properties or aggregate types. Another comment that requires further research is the lower influence of the temperature on the mixture K, the mixture that includes manufactured waste shingles. If that is shown true, the addition of manufactured waste shingles may improve the low temperature behavior of asphalt mixtures.

4.1.3 Tests for Strength Comparison

The remaining eight mixtures presented in Table 3-1, were tested using a loading rate of 3000mN/min, and a conditioning time of 1 hour. Testing was performed at 3 temperatures as previously indicated.

The maximum bending stress values for three replicates tested at each temperature are summarized in Table 4-12.

Table 4-12 Maximum bending stress for mixtures A,B,F,G,H,I,L,M

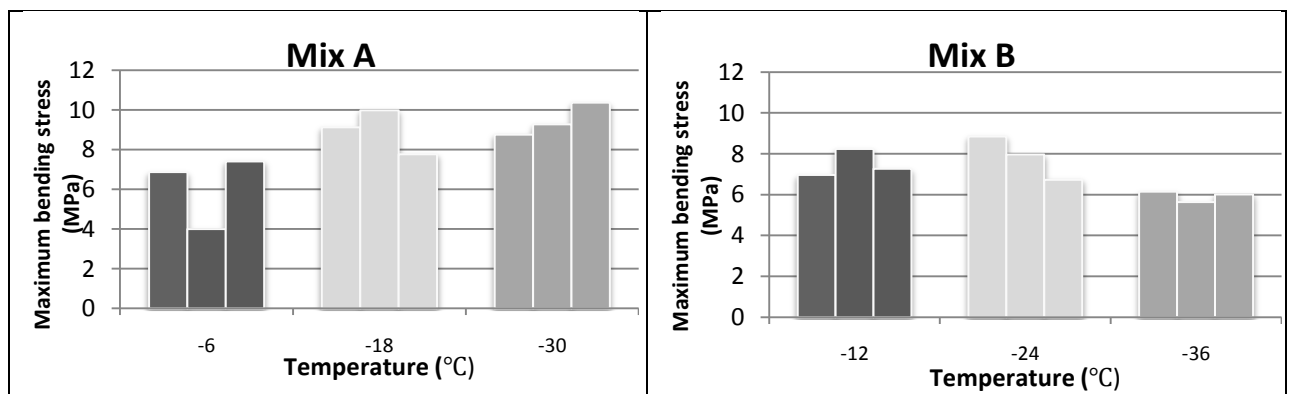
Temperature (°C)	Mix A Maximum Bending Stress (MPa)			Temperature (°C)	Mix B Maximum Bending Stress (MPa)		
	Beam #1	Beam #2	Beam #3		Beam #1	Beam #2	Beam #3
-6	6.88	4.00	7.41	-12	6.97	8.24	7.27
-18	9.13	9.99	7.77	-24	8.85	7.97	6.73
-30	8.76	9.28	10.37	-36	6.15	5.64	6.02

Temperature (°C)	Mix F Maximum Bending Stress (MPa)			Temperature (°C)	Mix G Maximum Bending Stress (MPa)		
	Beam #1	Beam #2	Beam #3		Beam #1	Beam #2	Beam #3
-12	6.25	6.02	6.09	-6	6.98	8.5	7.27
-24	7.35	7.31	7.22	-18	8.02	7.74	6.6
-36	4.75	4.55	4.17	-30	5.23	5.55	5.38

Temperature (°C)	Mix H Maximum Bending Stress (MPa)			Temperature (°C)	Mix I Maximum Bending Stress (MPa)		
	Beam #1	Beam #2	Beam# 3		Beam #1	Beam #2	Beam #3
-6	6.73	8.04	6.88	-12	7.91	6.28	8.49
-18	8.15	7.41	7.6	-24	8.14	8.81	8.37
-30	4.63	4.83	6.83	-36	6.2	5.45	5.76

Temperature (°C)	Mix L Maximum Bending Stress (MPa)			Temperature (°C)	Mix M Maximum Bending Stress (MPa)		
	Beam #1	Beam #2	Beam #3		Beam #1	Beam #2	Beam #3
-24	10.11	7.86		-6	7.38	6.07	9.5
-36	6.05	6.38		-18	8.03	7.56	7.56
				-30	6.71	6.69	5.47

The results are also plotted in Figure 4-8.



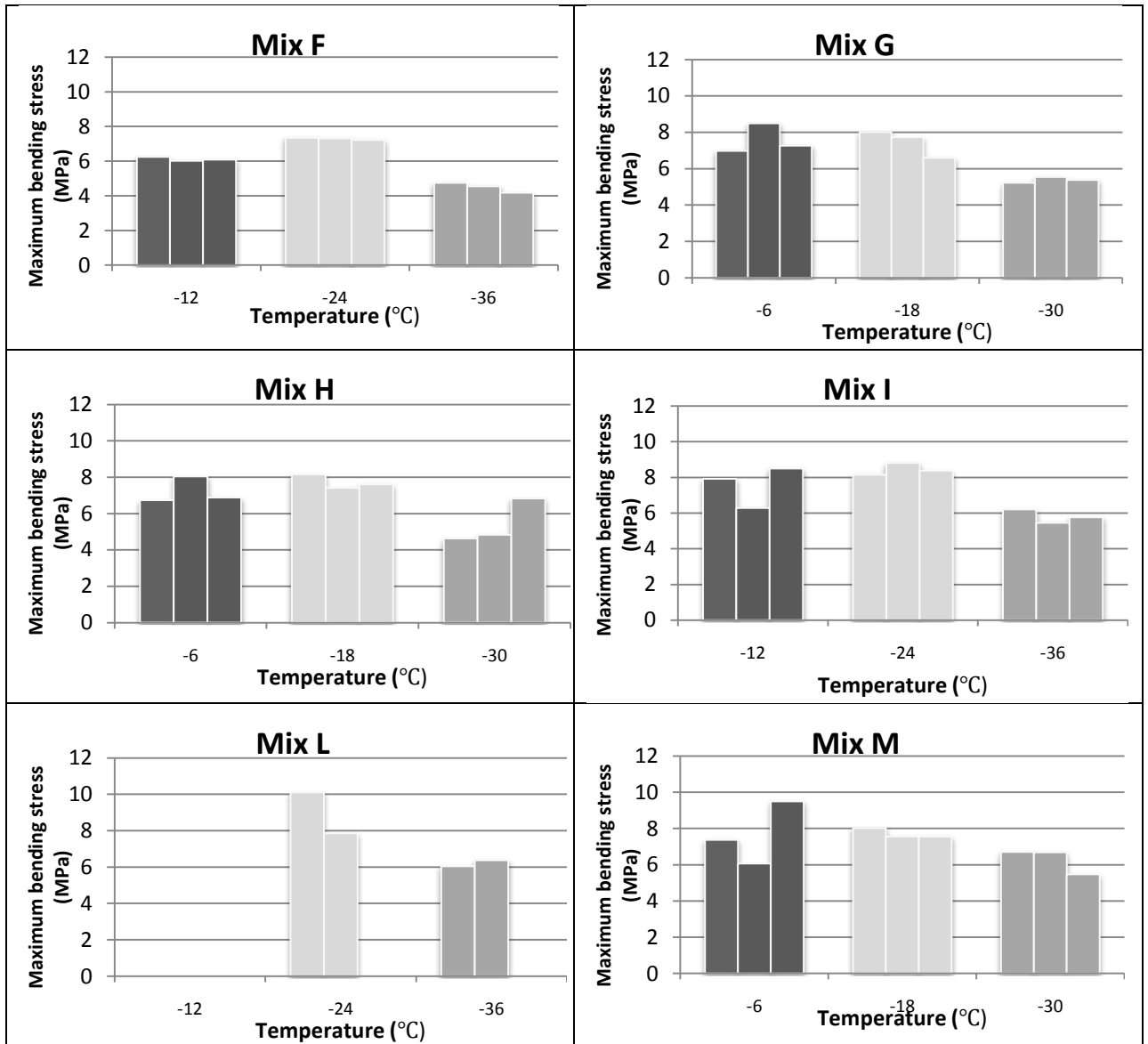


Figure 4-8 Maximum bending stress for mixtures A,B,F,G,H,I,L,M

Some trends are noticed in the data. The maximum bending stress increases from the higher temperature to the intermediate level. A further decrease of temperature to the lowest level results in decrease of the maximum bending stress compared.

To better understand these trends, a statistical analysis was performed. An analysis of variance with replication on the results presented above was used to investigate the effect of factors such mixture and temperature.

Table 4-13 below shows the result of the ANOVA.

Table 4-13 Analysis of Variance for maximum bending stress

Source	DF	SS	MS	F	P
mix	6	16.284	2.7140	2.40	0.0439
temp	2	42.237	21.1187	18.67	0.0000
mix*temp	12	21.434	1.7861	1.58	0.1351
Error	42	47.496	1.1309		
Total	62	127.451		Grand Mean 6.9824	CV 15.23

From Table 4-13 above, it can be seen that the temperature is a significant factor with a p-value of 0. The test discerns between the mixtures too, the mixture factor is significant with a p-value of 0.0439. However it is more difficult to quantify the difference between the mixtures, because their properties depend on the constituents and mix design. But it's promising that mixtures that do not look similar present different strength values.

The effects were further investigated by using a Tukey Honest Significant Difference (HSD) multiple comparisons for each factor. The all-pairwise multiple comparisons procedure, is used to compare the means of the different levels of a main effect or interaction.

Table 4-14 below shows the HSD comparison of the maximum bending stress for different mixtures.

Table 4-14 Tukey HSD All-Pairwise Comparisons Test of maximum bending stress for mix

Mix	Mean	Homogeneous Groups
A	7.7322	X
I	7.2678	XY
M	7.2189	XY
B	7.0933	XY
G	6.8078	XY
H	6.7889	XY
F	5.9678	Y

Alpha 0.05 Standard Error for Comparison 0.5013
 Critical Q Value 4.377 Critical Value for Comparison 1.5516
 Error term used: Error, 42 DF

There are 2 groups (X and Y) in which the means are not significantly different from one

another for the mixtures included in these groups. This may be explained by the not so different mixture composition.

Different homogenous group means that the temperature level offer significantly different results. Table 4-15 below shows the HSD comparison of the fracture strength for different temperature levels.

Table 4-15 Tukey HSD All-Pairwise Comparisons Test of maximum bending stress for temperature

<u>Temperature</u>	<u>Mean</u>	<u>Homogeneous Groups</u>
intermediate	7.9195	X
low	7.1029	Y
high	5.9248	Z

Alpha 0.3282 0.05 Standard Error for Comparison

Critical Q Value 0.7975 3.437 Critical Value for Comparison

Error term used: Error, 42 DF

From Table 4-15 above it can be seen that each testing temperature appeared to have a different effect on the maximum bending stress result. Each group, X, Y, Z has a different mean at a different testing temperature.

4.2 Indirect Tension Test

The same 11 mixtures were tested at temperatures similar to those used for bending beam strength testing. Three replicates were used for each set of mixture and temperature. The test were performed using the standard crosshead displacement rate of 12.5mm/min

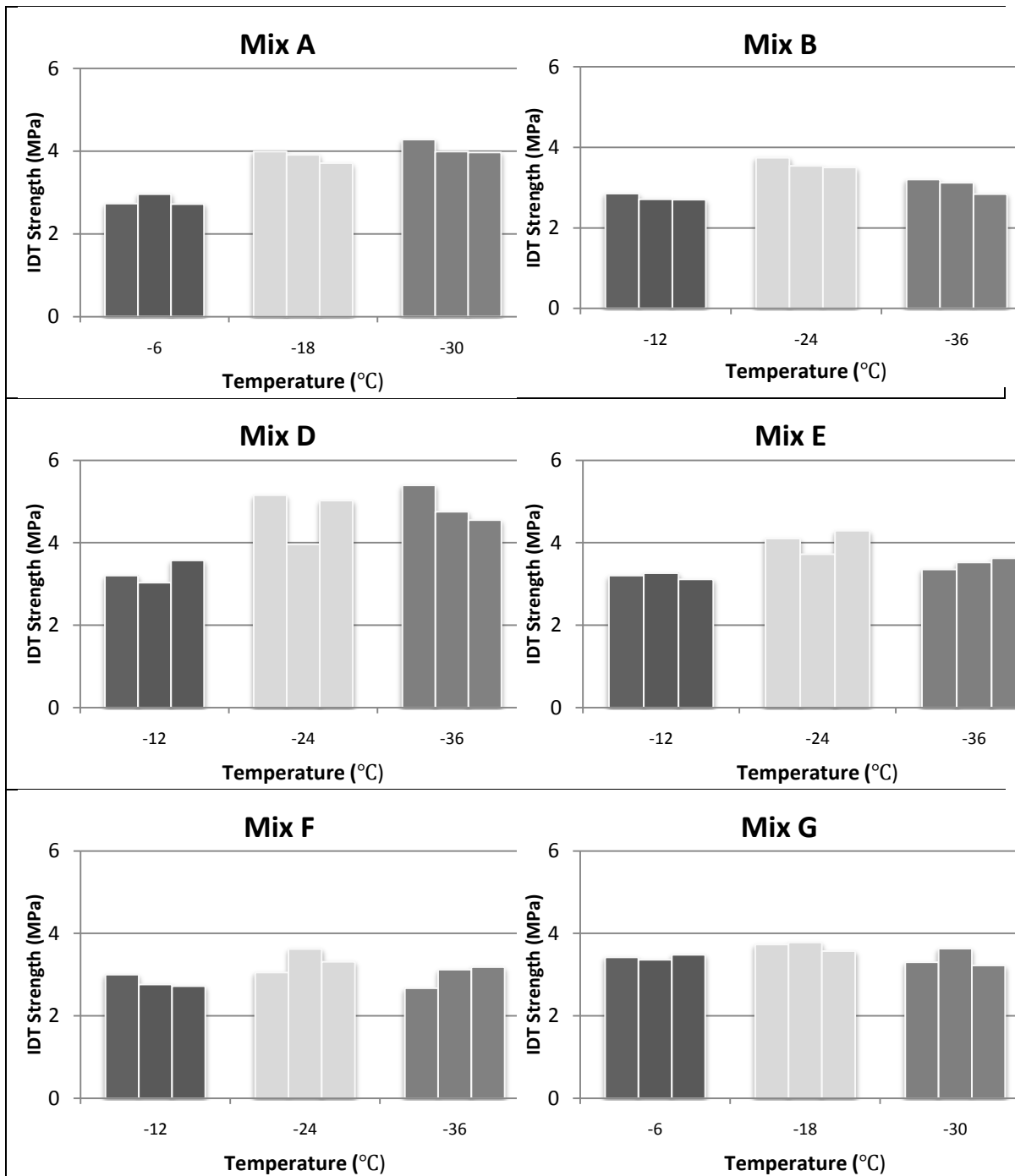
Table 4-16 presents the tensile strength values for all mixtures tested. The tests were run without using extensometers and the values were corrected using equation 2.2. It must be noted that this equation is applicable for stress values measured in kips and the test result were recorded in MPa. Therefore, the readings were transformed in kips, corrected and

transformed back to the original units. Three replicates for each temperature for each mixture were tested.

Table 4-16 IDT Strength for all mixtures

Mixture	Temperature (°C)	Tensile Strength, corrected (MPa)				CV(%)
		Sample 1	Sample 2	Sample 3	Average	
A	-6	2.73	2.96	2.72	2.80	4.87
	-18	3.99	3.91	3.71	3.87	3.74
	-30	4.28	3.99	3.97	4.08	4.19
B	-12	2.85	2.71	2.70	2.75	3.10
	-24	3.74	3.54	3.50	3.59	3.58
	-36	3.20	3.12	2.84	3.05	6.28
D	-12	3.20	3.03	3.57	3.27	8.48
	-24	5.15	3.96	5.02	4.71	13.90
	-36	5.39	4.75	4.55	4.90	9.02
E	-12	3.20	3.26	3.11	3.19	2.27
	-24	4.10	3.72	4.29	4.04	7.28
	-36	3.35	3.52	3.62	3.50	3.94
F	-12	3.00	2.76	2.72	2.83	5.45
	-24	3.05	3.62	3.31	3.33	8.61
	-36	2.67	3.12	3.18	2.99	9.33
G	-6	3.42	3.36	3.48	3.42	1.65
	-18	3.73	3.78	3.57	3.69	3.05
	-30	3.30	3.63	3.22	3.38	6.49
H	-6	3.51	3.23	3.19	3.31	5.37
	-18	3.47	3.79	4.17	3.81	9.11
	-30	3.37	3.60	4.17	3.72	11.13
I	-12	3.57	3.13	3.54	3.41	7.17
	-24	3.63	4.13	4.11	3.96	7.26
	-36	3.70	3.78	4.25	3.91	7.56
K	-6	2.66	2.77	2.77	2.73	2.34
	-18	3.63	2.91	3.41	3.31	11.20
	-30	3.37	2.84	3.10	3.10	8.59
L	-12	3.70	3.34	3.17	3.40	7.97
	-24	3.61	3.95	3.42	3.66	7.34
	-36	3.98	3.90	3.51	3.80	6.69
M	-6	3.06	3.24	3.34	3.21	4.40
	-18	4.15	3.71	3.55	3.80	8.07
	-30	3.83	3.29	3.11	3.41	10.96

The results are also plotted in Figure 4-9



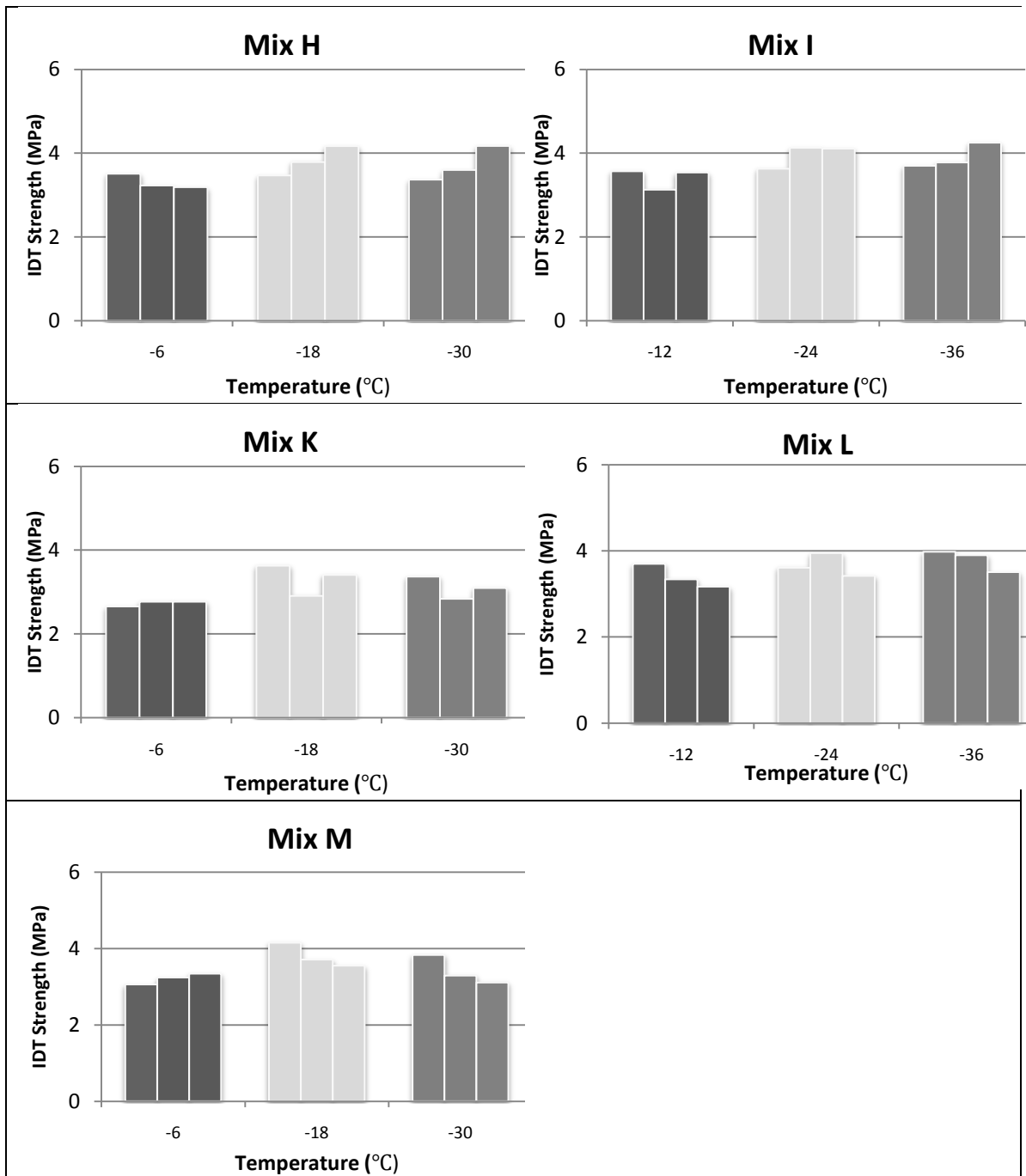


Figure 4-9 IDT Strength for all mixtures

Some trends are noticed in the data. The maximum bending stress increases from the higher temperature to the intermediate level. A further decrease of temperature does not result into visible and similar variation of the tensile strength for the tested mixtures. For

Critical Q Value 4.675 Critical Value for Comparison 0.5121
 Error term used: Error, 86 DF

There are 4 groups W,X,Y,Z in which the means are not significantly different from one another.

Table 4-19 Tukey HSD All-Pairwise Comparisons Test of IDT Strength for temperature

Temperature	Mean	Homogeneous Groups
intermediate	3.7979	X
low	3.6212	X
high	3.1212	Y

Alpha 0.05 Standard Error for Comparison 0.0809
 Critical Q Value 3.373 Critical Value for Comparison 0.1930
 Error term used: Error, 86 DF

From Table 4-19 above it can be seen that the intermediate and the low temperature (homogeneous group X) do not appear to have a different effect on the maximum bending stress value. This conclusion is similar to what was observed in Figure 4-9.

4.3 Direct Tension Test

A limited number of tests were performed using the DT test. Table 4-20 presents the Tensile strength values measured. Two replicates were tested for the temperature at which the test was performed.

Table 4-20 DT Tensile Strength for mixture D,E,K

Mixture	Temperature (°C)	Tensile Strength (MPa)		
		Sample1	Sample 2	Average
D	-36	4.09	4.33	4.21
E	-36	3.17	2.95	3.06
K	-30	3.33	3.34	3.335

4.4 Thermal Stress Restrained Specimen Test (TSRST)

Due to low availability of material for this test, only three different mixtures, D, E, and K were utilized. Two replicates were tested for each mixture. Since the temperature varies during the test fracture of the specimens occurs at different temperatures. Table 4-21 summarizes the fracture temperature and the fracture stress for the three mixtures.

Table 4-21 TSRST Tensile Strength for mixture D,E,K

Mixture	Sample 1		Sample 2	
	Tensile strength (MPa)	Temperature (°C)	Tensile strength (MPa)	Temperature (°C)
D	2.6	-34	2.41	-33.2
E	3.66	-34.6	3.28	-33.5
K	2.47	-27	2.51	-29.5

Please note that for TSRST, fracture occurred at temperatures higher than the lowest temperature used in BBS, IDT, and DT testing. As a result, TSRST data was not used in the comparison analysis.

4.5 Comparison of the Results from BBS, IDT and DT Testing

Two sets of comparisons were performed. For the first one, called measured values, the results were not transformed and were compared as they were recorded, except for the IDT correction (equation 2.2).

In the second set, equivalent results obtained by transforming the recorded set of values using the Weibull formulas presented in paragraph 2.2.2, were used. These formulas consider the size of the sample and the type of the test. Fracture strength for a unitary volume was calculated for all tests, and in addition, the bending fracture strength obtained with the BBR was transformed in a tensile strength. A t-test paired two sample for means was used to compare the results.

4.5.1 Measured Values

The average values for the fracture stress for the three tests are presented in Table 4-22.

Table 4-22 Fracture Strength, measured values

Mixture	Temperature (°C)	IDT	BBS	DT
A	-6	2.80	6.1	
	-18	3.87	8.97	
	-30	4.08	9.47	
B	-12	2.75	7.49	
	-24	3.59	7.85	
	-36	3.05	5.93	
D	-12	3.27		
	-24	4.71	10	
	-36	4.90	7.2	4.21
E	-12	3.19		
	-24	4.04	7.47	
	-36	3.50	4.7	3.06
F	-12	2.83	6.12	
	-24	3.33	7.29	
	-36	2.99	4.49	
G	-6	3.42	7.58	
	-18	3.69	7.45	
	-30	3.38	5.39	
H	-6	3.31	7.22	
	-18	3.81	7.72	
	-30	3.72	5.43	
I	-12	3.41	7.56	
	-24	3.96	8.44	
	-36	3.91	5.80	
K	-6	2.73		
	-18	3.31	5.85	
	-30	3.10	4.85	3.335
L	-12	3.40		
	-24	3.66	8.98	
	-36	3.80	6.21	
M	-6	3.21	7.65	
	-18	3.80	7.72	
	-30	3.41	6.29	

The IDT and BBS tests were run in similar temperature conditions, with 3 replicates for each mixture. For DT test just two replicates at one temperature were run.

Figure 4-10 shows the strength obtained through the three testing methods.

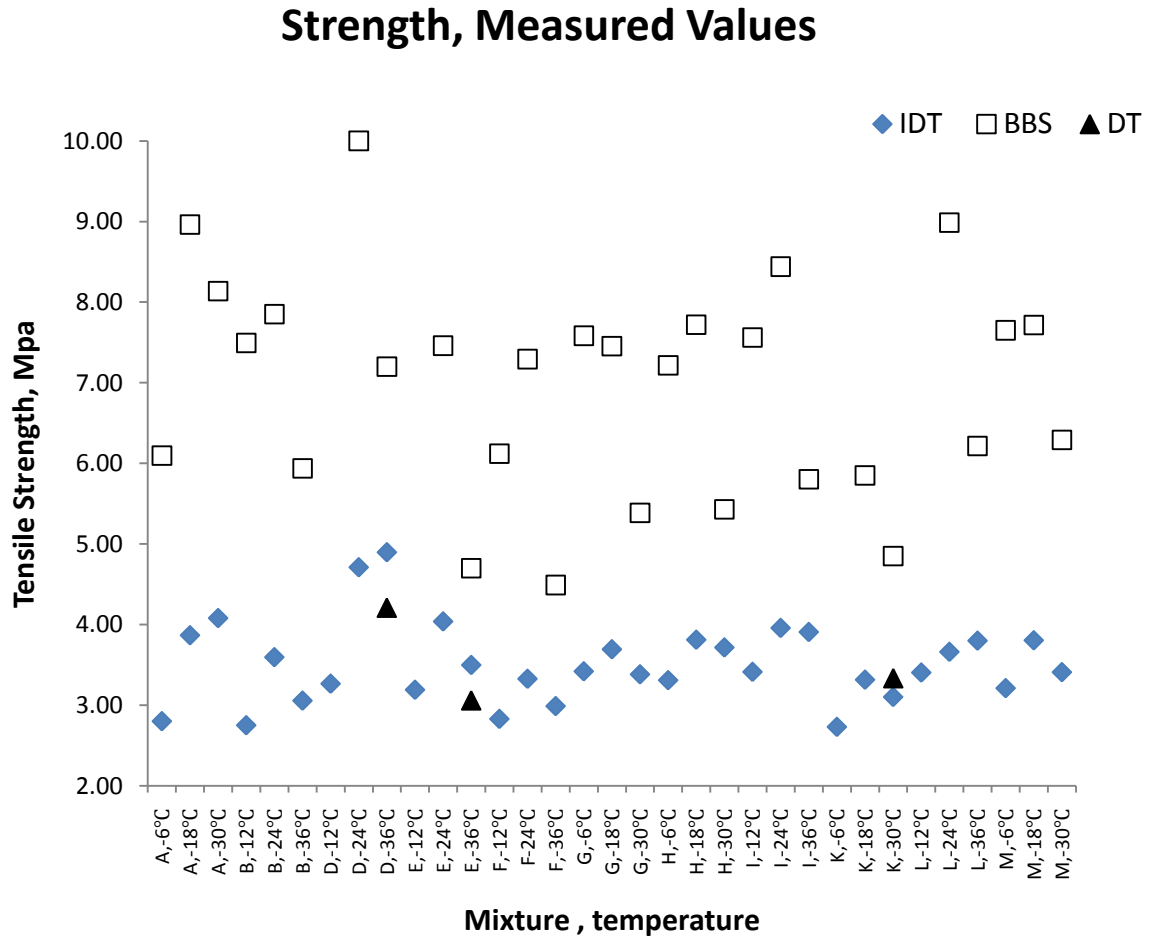


Figure 4-10 Strength, measured values

As seen in Figure 4-10, the BBS values are higher than the other two sets of data. The difference between the IDT and DT values is smaller and in two cases IDT gives higher strength and in one case the DT test.

4.5.2 Statistical Analysis for the Measured Values

The statistical analysis for the fracture strength data was meant to determine whether there were differences between different tests. A t-Test paired two sample for means was

run in Microsoft Excel. The test was run three times, comparing IDT with BBR results, IDT with DT results and BBR and DT results. In each case, the null hypothesis H_0 stated that there is no difference between the tests, and the alternative hypothesis H_a stated that the tests give different results. Because no direction for the difference is specified, a two-sided alternative was chosen. The critical p value is 0.01.

Table 4-23 t-Test Paired Two Sample for Means, measured values

t-Test: Paired Two Sample for Means			t-Test: Paired Two Sample for Means		
	<i>IDT</i>	<i>BBS</i>		<i>IDT</i>	<i>DT</i>
Mean	3.5630	6.96172	Mean	3.8315	3.53333
Variance	0.2564	1.84495	Variance	0.8905	0.36163
Observations	29.0000	29.00000	Observations	3.0000	3.00000
Pearson Correlation	0.5039		Pearson Correlation	0.9054	
Hypothesized Mean Difference	0.0000		Hypothesized Mean Difference	0.0000	
df	28.0000		df	2.0000	
t Stat	15.4231		t Stat	1.0902	
P(T<=t) one-tail	0.0000		P(T<=t) one-tail	0.1947	
t Critical one-tail	1.7011		t Critical one-tail	2.9199	
P(T<=t) two-tail	0.0000		P(T<=t) two-tail	0.3894	
t Critical two-tail	2.0484		t Critical two-tail	4.3026	
t-Test: Paired Two Sample for Means					
	<i>BBS</i>	<i>DT</i>			
Mean	5.5833	3.53333			
Variance	1.9658	0.36163			
Observations	3.0000	3.00000			
Pearson Correlation	0.9850				
Hypothesized Mean Difference	0.0000				
df	2.0000				
t Stat	4.3499				
P(T<=t) one-tail	0.0245				
t Critical one-tail	2.9199				
P(T<=t) two-tail	0.0490				
t Critical two-tail	4.3026				

It can be observed in Table 4-23 that, when BBS test results were compared with IDT, the two-tail p-value is smaller than the critical p value, which means the alternative hypothesis is true and there is a difference between the two tests. For the other

comparisons, the two-tail p value is bigger than the critical p value, which means that there is no difference between IDT and DT or BBS and DT results.

4.5.3 Equivalent Values

The equivalent results, obtained by transforming the recorded set of values using the Weibull formulas as described before, are presented in Table 4-24.

Table 4-24 Equivalent unitary volume Tensile Strength

Mixture	Temperature (°C)	Equivalent unitary volume Tensile Strength, MPa		
		IDT	Transformed BBS	DT
A	-6	4.91	5.30	
	-18	6.79	7.79	
	-30	7.16	8.23	
B	-12	4.83	6.51	
	-24	6.31	6.82	
	-36	5.36	5.16	
D	-12	5.73		
	-24	8.27	8.69	
	-36	8.60	6.26	6.93
E	-12	5.60		
	-24	7.09	6.49	
	-36	6.14	4.08	5.04
F	-12	4.96	5.32	
	-24	5.84	6.34	
	-36	5.24	3.90	
G	-6	6.00	6.59	
	-18	6.48	6.48	
	-30	5.94	4.68	
H	-6	5.81	6.27	
	-18	6.69	6.71	
	-30	6.52	4.72	
I	-12	5.99	6.57	
	-24	6.95	7.34	
	-36	6.86	5.04	
K	-6	4.79		
	-18	5.82	5.50	
	-30	5.44	4.14	5.49
L	-12	5.97		
	-24	6.43	7.81	
	-36	6.67	5.40	
M	-6	5.63	6.65	
	-18	6.68	6.71	
	-30	5.98	5.47	

Figure 4-11 reveals a much smaller difference between the IDT and the BBS results than in Figure 4-10. More than this, before BBS tests gave higher results in all cases, but after the transformation, the number of test for which BBS got higher value is equal to the number of test for which IDT strength is higher.

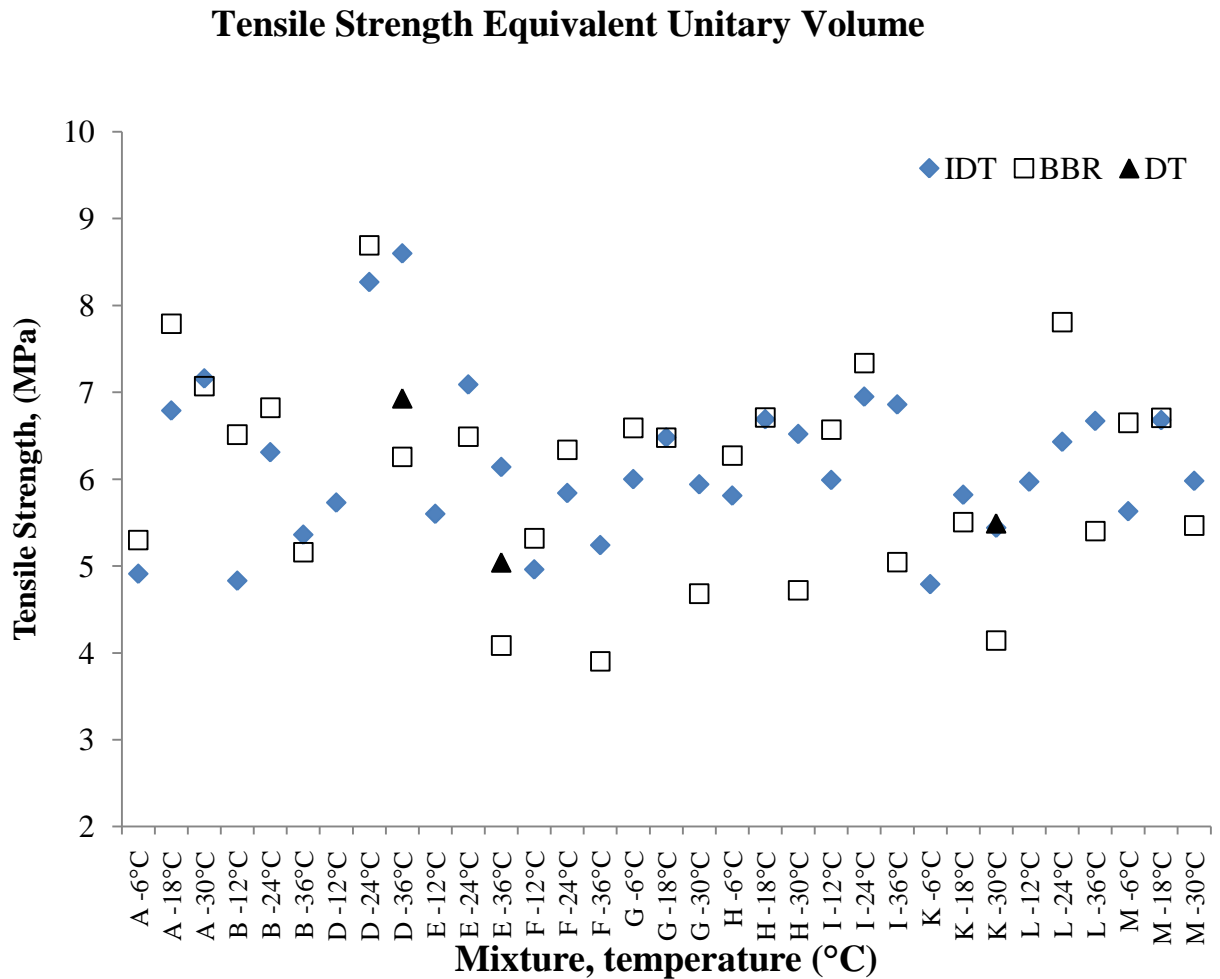


Figure 4-11 Tensile strength, equivalent unitary volume

Another way to compare two methods that are designed to measure the same property is the Bland Altman plot, Figure 4-12.

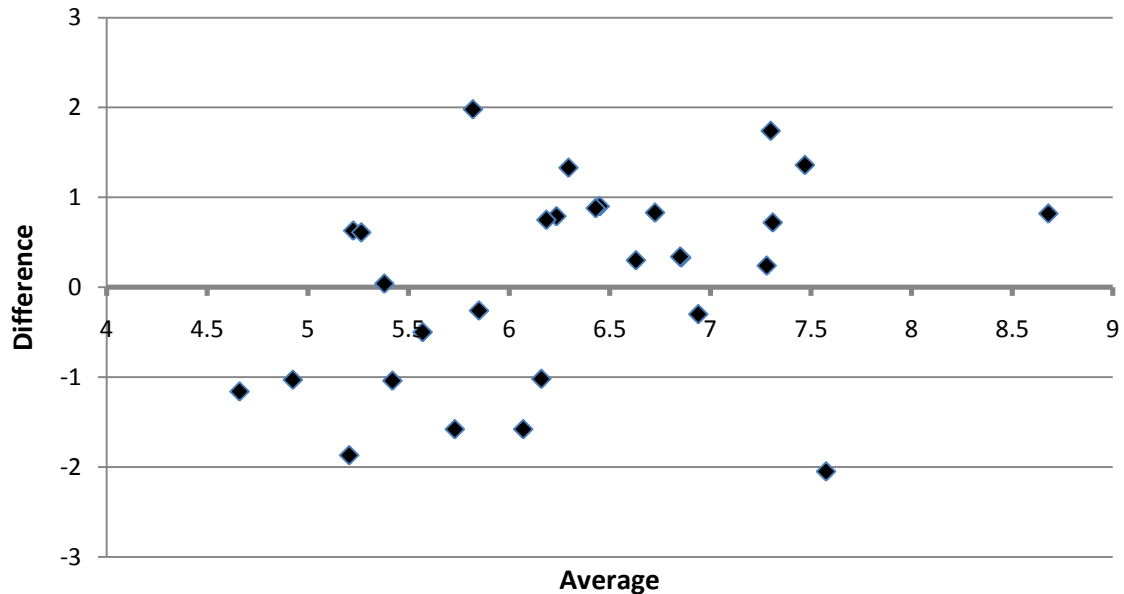


Figure 4-12 Bland-Altman plot

As seen in the plot, the mean of the tensile strength equivalent volume unit measured using the IDT and BBS method for the same material and temperature is assigned as the x-axis value, and the difference between the two values is assigned as the y-axis value. The points on the Bland-Altman plot are scattered all over the place, above and below zero. This suggests that there is no consistent bias of one approach versus the other, and that there is an acceptable level of agreement between the two different testing methods.

4.5.4 Statistical Analysis for Equivalent Values

The statistical analysis for the equivalent unitary volume tensile strength data was meant to determine whether there were differences between tests. The results of the t-Test paired two samples for means are presented in Table 4-25. The test was run three times, comparing IDT with BBR results, IDT with DT results and BBR and DT results. In each case, the null hypothesis H_0 stated that there is no difference between the tests, and the alternative hypothesis H_a stated that the tests give different results.

Because no direction for the difference is specified, a two-sided alternative was chosen. The critical p-value is 0.01.

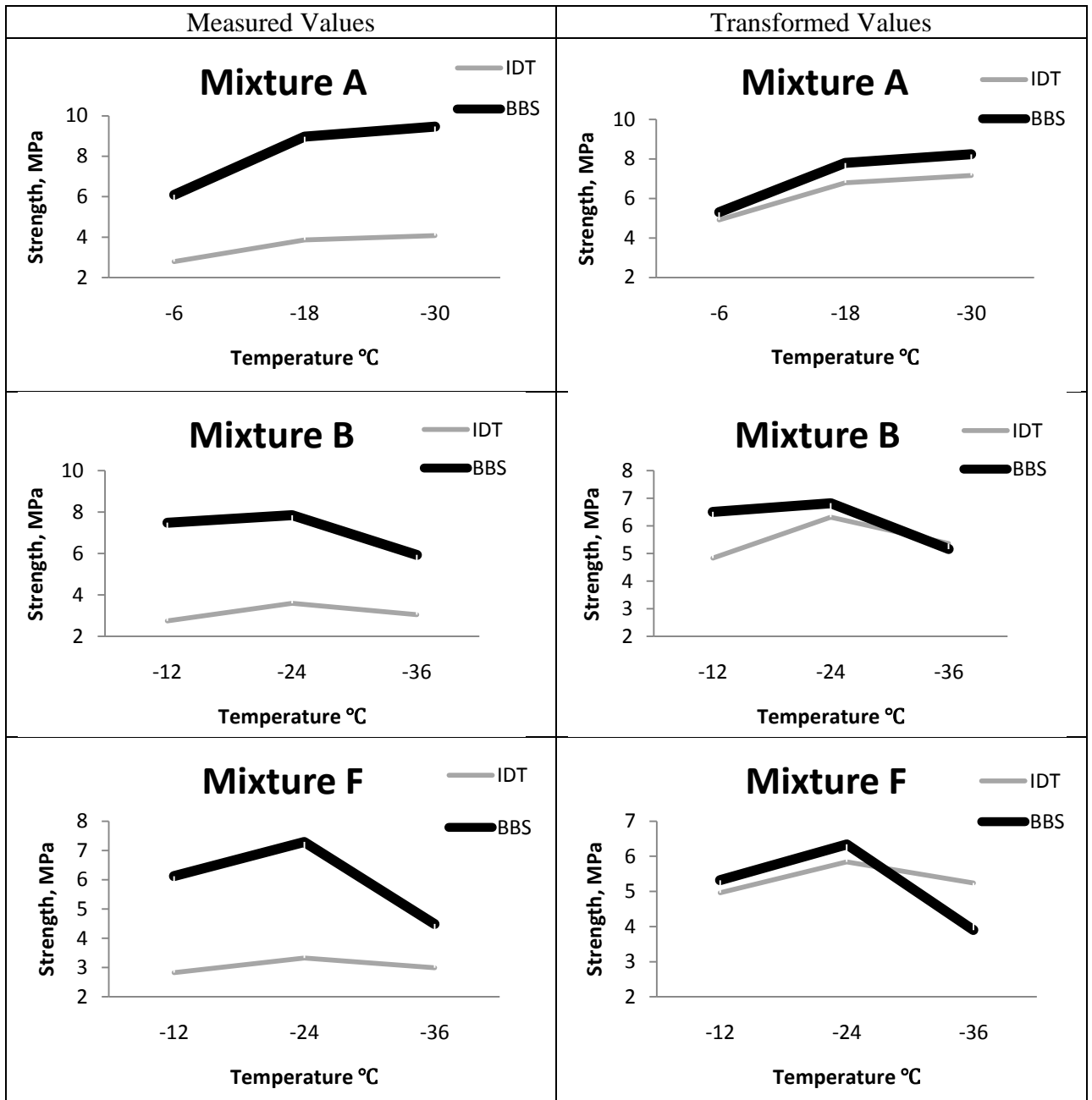
Table 4-25 t-Test Paired Two Sample for Means, equivalent values

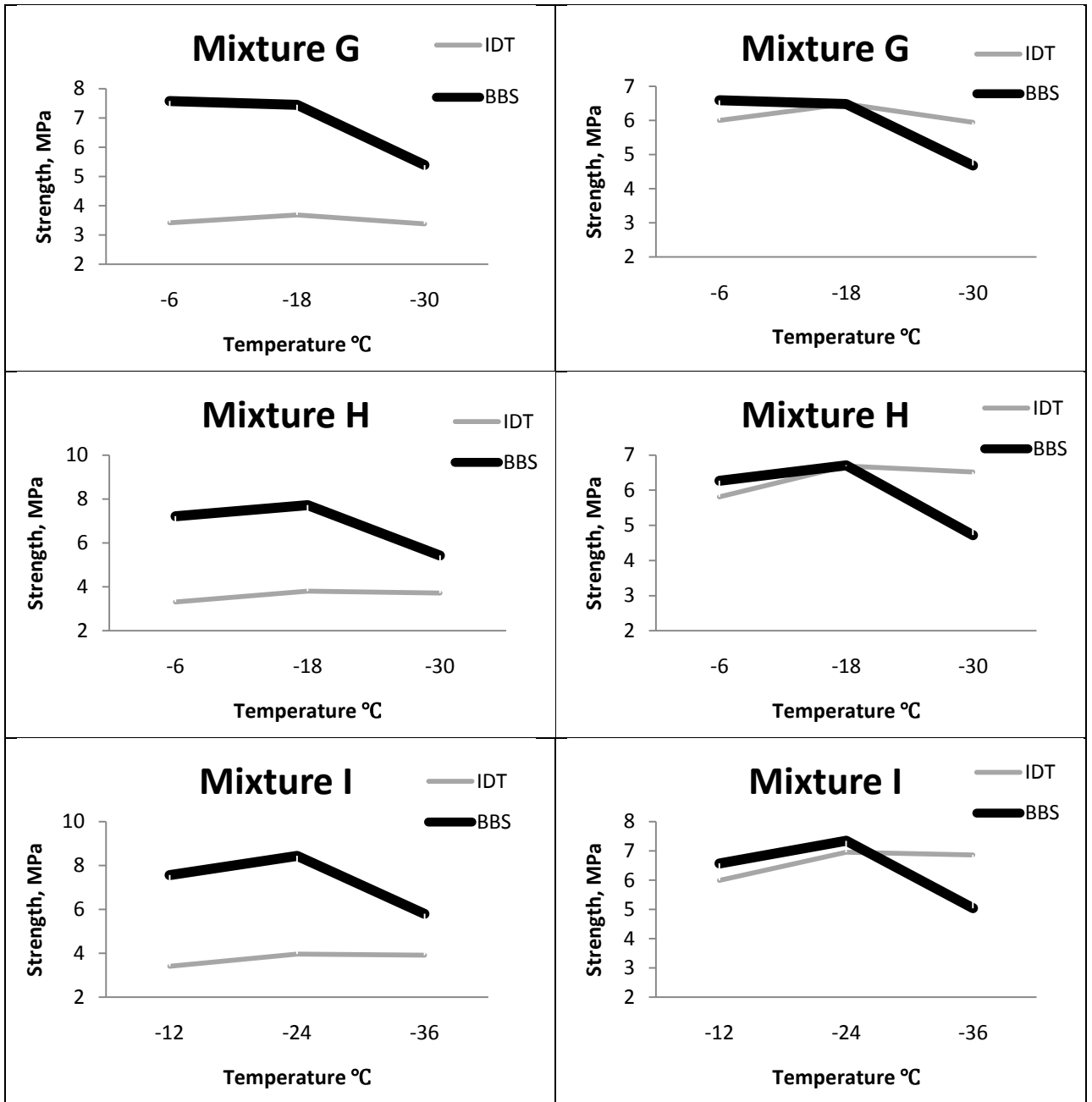
t-Test: Paired Two Sample for Means			t-Test: Paired Two Sample for Means		
	<i>IDT unit equiv</i>	<i>BBS unit equiv</i>		<i>IDT unit equiv</i>	<i>DT unit equiv</i>
Mean	6.2548	6.3309	Mean	6.7261	5.8212
Variance	0.7903	1.5256	Variance	2.7444	0.9779
Observations	29.0000	29.0000	Observations	3.0000	3.0000
Pearson Correlation	0.5040		Pearson Correlation	0.9035	
Hypothesized Mean Difference	0		Hypothesized Mean Difference	0	
df	28.0000		df	2.0000	
t Stat	0.97636		t Stat	1.7955	
P(T<=t) one-tail	0.16862		P(T<=t) one-tail	0.1072	
t Critical one-tail	1.7011		t Critical one-tail	2.9199	
P(T<=t) two-tail	0.3372		P(T<=t) two-tail	0.2144	
t Critical two-tail	2.0484		t Critical two-tail	4.3026	
t-Test: Paired Two Sample for Means					
	<i>DT unit equiv</i>	<i>BBS unit equiv</i>			
Mean	5.8212	4.828			
Variance	0.9779	1.5328			
Observations	3.0000	3.0000			
Pearson Correlation	0.9787				
Hypothesized Mean Difference	0				
df	2.0000				
t Stat	-5.0673				
P(T<=t) one-tail	0.01840				
t Critical one-tail	2.9199				
P(T<=t) two-tail	0.0368				
t Critical two-tail	4.30265				

It can be seen that in all cases the two-tail P value is bigger than the critical p-value. That means the null hypothesis is true and there is no difference between the BBR test results and the other two tests.

4.5.5 Trend Comparison

Figure 4-13 presents a comparison of the trend of the strength results for the measured values (Table 4-22), left column, and for the transformed values (Table 4-24), right column, for the seven mixture that had the complete set of results.





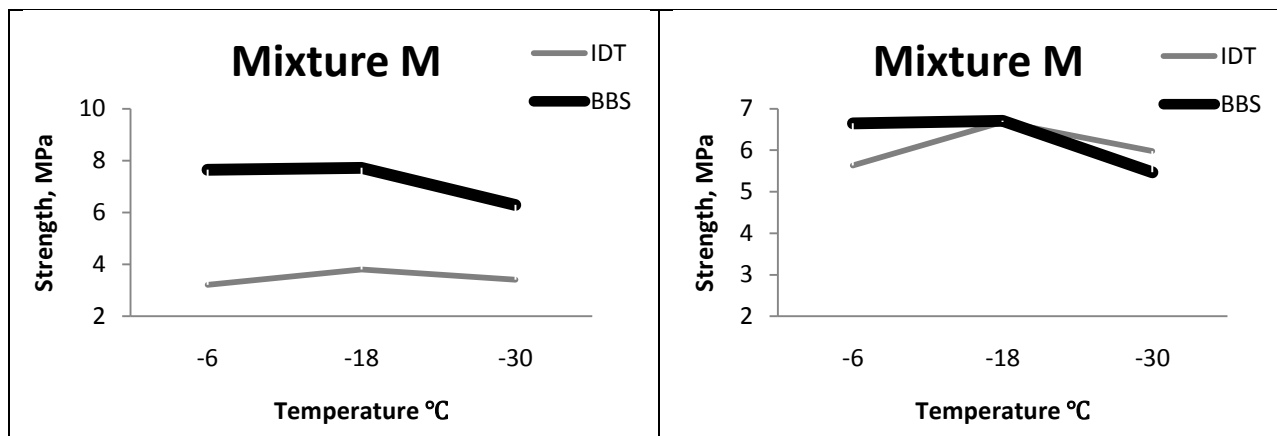


Figure 4-13 Strength trend

As seen in Figure 4-13 mixture A is the only one that presents a continuous fracture strength increase, starting from the highest testing temperature to the lowest one for both testing methods.

Mixture A, Novachip, is commonly used as a surface treatment of the pavement. It is possible that the PG grade of the binder or the mix design was different, so the strength did not reach the peak at the intermediate temperature. However, both tests have observed the same behavior.

For the other six mixtures tested at three temperatures, the strength increases when the temperature decreases from the highest to the intermediate value. At the lowest temperature, the strength decreases for all the mixtures, for both considered tests, IDT and BBS.

All this trend analysis is valid for the strength-transformed values too. In this case it is visible again the smaller difference between the values obtained through the two different tests.

To investigate the performance of the new developed testing method different tools were used.

It has been shown that even without any transformation the new method, BBS, and the standardized one IDT provide a similar trend for the results. Still the results are statistically different, based probably on the huge difference in volume (73 times), between the two samples.

By including in the analysis the Weibull transformation for size effect and type of test, there is no more statistical difference between the different test procedures; hence, the BBS may be used to determine the fracture strength.

Chapter 5.

Summary and Conclusions

Both the asphalt mixture creep stiffness and strength are needed in the AASHTO Mechanistic Empirical Pavement Design Guide low temperature algorithm to predict low temperature performance. A procedure for obtaining creep stiffness by testing thin asphalt mixtures beams using a Bending Beam Rheometer was developed by Marasteanu et al. (18) This thesis continue that work and investigate the possibility of performing strength tests on thin mixtures beams with the slightly modified Bending Beam Rheometer.

In the first part of this thesis, the literature review, different strength tests used for asphalt mixtures, general material properties, and considerations related to size effect and the equivalency between different procedures are presented.

The experimental part starts with the sample preparation and the test matrix for the considered tests. The IDT standardized procedure (2) is performed on eleven mixtures. For three mixtures, DT and TSRST test are performed too. Then, on the same eleven mixtures three sets of tests are performed using the proposed method called Bending Beam Strength (BBS):

- The first set of tests is performed to investigate the reliability and reproducibility of BBS testing method, and the validity of the measuring concept. Weibull modulus is calculated as part of the analysis.
- The second set of tests is used to investigate the joint effect of temperature, conditioning time and loading rate, on the measured strength of three different mixtures, by using a 2^3 factorial design. At 1 % level the temperature is a significant factor for these mixtures. The conditioning time is not significant, and

the loading rate is significant just in one case. No interaction was found between the factors.

- The third set consists of tests performed on a second group of eight mixtures using the same loading rate and conditioning time at three temperatures. The PG grade of the binder used in each mix design was used to select the temperatures. An analysis of variance with replication is used to use the effect of factors such mixture and temperature.

Further the effects are investigated by using a Tukey Honest Significant Difference (HSD) multiple comparisons for each factor.

The results obtained thru different testing methods are then compared. The t- Test paired two samples for means using the measured values shows that the IDT and BBS results are statistically different.

A second comparison is presented. The measured values were transformed taking into account the size of the samples and the testing method difference. The Weibull theory related to the size effect and the equivalency between bending test and direct tension tests are utilized. The t- Test paired two samples for means, performed on the equivalent values obtained after transformation, shows no statistical difference between the BBS and the other tests results. A Bland-Altman plot confirms this conclusion.

The last set of plots presents a comparison of the trend of the strength results for the measured values and for the transformed values. A similar tendency is observed for all mixtures. It can be noticed also that BBS differentiates better between the intermediate and the lowest temperature than the IDT.

From the results presented in this thesis, it can be concluded that the BBS strength values are similar to the values obtained with other test methods. Therefore, BBS may offer a much simpler and cost effective way to determine low temperature strength of asphalt mixtures.

Bibliography

1. *Development of a simple test to determine the low temperature creep compliance of asphalt mixture.* **Marasteanu, M.O., Velasquez, R., Zofka, A., Cannone Falchetto, A.,** s.l. : Transportation Research Board of the National A, 2009, Vols. IDEA Program Final Report, NCHRP-133,.
2. T 322-03: Determining the Creep compliance and Strength of HOT-Mix Asphalt(HMA) Using the Indirect Tensile Test Device. *Standard Specification for Transportation Materials and Methods of Sampling and Testing, 26th Edition.* Washington DC : American Association of State Highway and transportation Officials, 2006.
3. *Standard test method for Thermal Strss Restrained Specimen Tensile Strength.* former TP10-93, deleted in 2000.
4. **Bolzan, P., Huber, G.,** Direct Tension Test Experiments. *Strategic Highway Research Program, SHRP-A-641.* Washington DC : National Research Council, 1993.
5. *A New Method to Determine the Tensile Strength of Concrete.* **Carneiro, F.L.L.B.,** 1943, Vols. Proceedings of the 5th Meeting of the Brazilian Association for Technical Rules, 3rd Section.
6. *Methodes pour l'essai de traction de betons.* **Akazawa.T.** s.l. : Journal of the Japanese Civil Engineering Institute, 1943, Vol. Bulletin RILEM 16 Paris 1953.
7. **Hodros, G.** The evaluation of Poisson's ratio and the modulus of materials of a low tensile resistance by the Brazilian (indirect test) with particular reference to concrete. 1959. Vols. Aust. J. Appl. Sci. 10, pp243-268.
8. **Dongre, R., Sharma, M.G. and Anderson, D.A.** Development of Fracture Criterion for Asphalt Mixtures at Low Temperatures. *Transportation Research Record.* Washington DC : National Research Council, 1989. Vols. 1228, pp 94-105.
9. **Roque, R. and Buttlar, W.G.** The Development of a Measurement and Analysis System to Accurately Determine Asphalt Concrete Properties Using the Indirect Tensile Mode. *Association of Asphalt Paving Technologists.* 1992. Vols. 61, pp304-328.
10. **Christensen, D.W. and Bonaquist, R.F.** *Evaluation of Indirect Tensile Test (IDT) Procedures for Low-Temperature Performance of Hot Mix Asphalt, NCHRP Report 530.* Washington, D.C. : Transportation Research Board, 2004.
11. **W.F., Chen.** Double Punch Test for Tensile Strength of Concrete. s.l. : American Concrete Institute, 1970. Vol. 67.

12. **Farouki, O.T., Rolt, J.** *Feasibility of Using Sand/Sulphur/Bitumen Mixes in Highway Pavement Construction*. s.l. : The Chartered Institution of Highway & Transportation, 1985.
13. **Kiggundu, B., Roberts, L.** *Stripping in the HMA Mixtures: State of the Art and Critical Reviews of Test Methods; NCAT Report 88-02*. s.l. : National Center for Asphalt Technology, 1988.
14. *Field Control Test for Debonding of Asphaltic Concrete*. **Jimenez, R.A.** 1228, Washington DC : Transportation Research Record, 1989.
15. **Bolzan, P., Huber, G.** *Direct Tension Test Experiments, SHRP-A-661*. Washington DC : Strategic Highway Research Program, 1993.
16. AASHTO 321 Standard Method of Test for Determining the Fatigue Life of Compacted Hot-Mix Asphalt (HMA) Subjected to Repeated Flexural Bending. Washington DC : AASHTO, 2008.
17. T 313-06 Determining the Flexural Creep Stiffness of Asphalt Binder Using the Bending Beam Rheometer (BBR). *Standard Specification for Transportation Materials and Methods of Sampling and Testing, 26th Edition*. Washington DC : American Association of State Highway Officials, 2006.
18. **Marasteanu, M.O., et al.** *IDEA Program Final Report, NCHRP-133*. Minneapolis : s.n., 2009.
19. **Freeman, Jr. J.R. and Maupin, Jr. G.W.** *Simple test method for possible use in predicting the fatigue of asphaltic concrete*. Charlottesville, Virginia : Virginia Highway and Transportation Research Council, 1975.
20. **Velasquez, R.A.** *On the Representative Volume Element of Asphalt Concrete*, PhD Thesis. s.l. : University of Minnesota, 2009.
21. **Kim, Y.R., Lutif, J.E.S., Allen, D.H.** *Determining Representative Volume Element of Asphalt Concrete Mixtures Without Damage*. *Journal of the Transportation Research Board*. Washington DC : s.n., 2009. Vols. 2127, pp 52-89.
22. **Seo, Y., et al.** *Application of Digital Image Correlation Method to Mechanical Testing of Asphalt Aggregate Mixtures*. *Journal of the Transportation Research Board*. Washington : s.n., 2002. Vols. 1789, pp 169-172.
23. **Masad, E., Tashman, L., Samedavan, V., Little, D.,** *Micromechanics-Based Analysis of Stiffness Anisotropy in Asphalt Mixtures*. *J. Mat in Civ. Engrg.* 2002. Vols. 14, pp 374-383.
24. **Westinghouse Electric Corporation Astronuclear Laboratory.** *Theory and Structural Design Applications of Weibull Statistics*. Pittsburgh : s.n., 1970.
25. **Bazant, Zdenek and Planas, Jaime.** *Fracture and Size Effect in Concrete and Other Quasibrittle Materials*. Boca Raton : CRC Press, 1998.

26. **Cannon Instrument Company.** Cannon Bending-Beam Rheometer. *Instruction & Operation Manual.* 1998.
27. **Montgomery, D.C.** *Design and Analysis of Experiments.* New York : John Wiley & Sons, 1991.
28. **Askeland, Donald R. and Phulé, Pradeep P.** *The Science And Engineering Of Materials.* s.l. : Thomson, 2005.
29. *Evaluation of Low-Temperature Properties of HMA Mixtures.* **Sebaaly, P.E., Lake, A. and Epps, J.** s.l. : Journal of Transportation Engineering, 2002, Vol. November/December.
30. **Trantina, G. and Nimmer, R.** *Structural Analysis of Thermoplastic Components.* s.l. : McGraw-Hill, Inc., 1994.
31. *Physical Hardening of Asphalt Binders Relative to Their Glass Transition Temperatures.* **Anderson, A. and Marasteanu, M.O.** s.l. : Transportation research Record, Vols. 99-1547.
32. **Mitchell, W.B.** The Indirect Tension Test for Concrete. *Materials Research and Standards.* s.l. : American Society for Testing Materials, 1961. Vol. 1, 10.
33. **Weismann, S.L., et al.** Selection of Laboratory Test Specimen Dimension for Permanent Deformation of Asphalt Concrete Pavements. s.l. : TRB, 1999.
34. **Zofka, A.M.,.** Investigation of asphalt concrete behaviour using 3-point bending test. PhD thesis. s.l. : University of Minnesota, 2007.